Available online at www.sciencedirect.com
SCIENCE DIRECT®
Journal of Computational Physics 199 (2004) 126–149
JOURNAL OF COMPUTATIONAL PHYSICS
www.elsevier.com/locate/jcp

# On the application of lacunae-based methods to Maxwell's equations

S.V. Tsynkov *,[1]

*Department of Mathematics and Center for Research in Scientific Computation (CRSC), North Carolina State University, Box 8205, Raleigh, NC 27695, USA*

Received 22 July 2003; received in revised form 4 February 2004; accepted 5 February 2004
Available online 5 March 2004

**Abstract**

A straightforward application of the previously designed lacunae-based numerical methods to unsteady electromagnetic problems would encounter certain difficulties, as it may violate the continuity of the charges and currents, which is a necessary solvability condition for the Maxwell equations. In the paper, we prove existence of the special auxiliary charges and currents that satisfy the continuity equations identically. We also show that using such charges and currents as a part of the numerical procedure provides a clear and unobstructed venue toward implementation of the lacunae-based methods in electromagnetics.


*Keywords:* Electromagnetic waves; Continuity equation; Solenoidal currents; Partition of unity; Unsteady propagation; Unbounded domains; Truncation; Finite computational domain; Sharp aft fronts; Huygens' principle; Non-deteriorating method; Long-term numerical integration

## 1. Introduction

Lacunae-based methods have been built earlier for the scalar wave equation [1,2] and for the system of acoustics [3]. They enable non-deteriorating long-term integration of the corresponding equations driven by continuously operating compact sources, and, in a more complex environment, facilitate construction of highly accurate global artificial boundary conditions (ABCs) with only limited extent of temporal nonlocality.

To set the lacunae-based ABCs at the outer boundary of a finite computational domain, one first splits the original infinite-domain problem into the interior and auxiliary sub-problems. The interior problem is posed on the aforementioned bounded computational region, whereas the auxiliary problem is still posed

* Tel.: +1-919-515-1877; fax: +1-919-515-3798.
*E-mail address:* tsynkov@math.ncsu.edu (S.V. Tsynkov).
*URL:* http://www.math.ncsu.edu/~stsynkov.
[1] The author gratefully acknowledges support by AFOSR, Grant F49620-01-1-0187, and that by NSF, Grant DMS-0107146.

0021-9991/$ - see front matter 
doi:10.1016/j.jcp.2004.02.003

on the entire space. The two problems are connected to one another in such a way that the source terms of the auxiliary problem depend on the interior solution right inside the boundary, and the solution of the auxiliary problem right outside the boundary provides the required closure for the interior formulation, i.e., the ABCs. The key objective and key advantage of employing this decomposition is that in a number of interesting cases the auxiliary problem can be formulated so that its solutions would have lacunae. In other words, the auxiliary problem would satisfy the Huygens' principle, which characterizes certain hyperbolic PDEs in odd-dimension spaces. The presence of lacunae can be translated into an efficient non-deteriorating numerical algorithm for integrating the auxiliary problem, which, in turn, yields the ABCs whose restricted nonlocality in time does not come at the expense of introducing any approximations and/or simplifications to the original model, but rather reflects the fundamental properties of the corresponding solutions.

As, however, shown in Section 3 of the paper, a key obstacle for implementation of the lacunae-based methods in electromagnetics happens to be the necessary requirement of continuity for the charges and currents that drive the Maxwell equations. More precisely, using the lacunae-based integration in its original form [1–3] may violate the continuity, thus rendering the corresponding auxiliary problem unsolvable. In the paper, we prove existence of a special class of auxiliary currents and charges that satisfy the continuity requirement identically (solenoidal currents and zero charges). We also prove that employing the solenoidal auxiliary currents in the numerical procedure helps eliminate the foregoing hurdle and does allow for the use of lacunae-based algorithms in electromagnetics. This is the central theoretical conclusion of the paper, which is also corroborated in Section 5 by a series of numerical demonstrations. The computations of Section 5 are conducted for the cylindrically symmetric case, which helps us keep their overall cost low, while still preserving the vital three-dimensional effects. Besides, cylindrical symmetry leads to a rather simple algorithm for obtaining the solenoidal currents. Implementation of a more general algorithm will be reported in the forthcoming publication [4].

## 2. Maxwells equations and solenoidal currents

The propagation of electromagnetic waves in vacuum is governed by the Maxwell system of equations:

$$\begin{aligned} &\frac{1}{c}\frac{\partial \boldsymbol{H}}{\partial t} + \operatorname{curl}\boldsymbol{E} = -\frac{4\pi}{c}\boldsymbol{j}_{\mathrm{m}}, \quad \operatorname{div}\boldsymbol{H} = 4\pi\rho_{\mathrm{m}}, \\ &\frac{1}{c}\frac{\partial \boldsymbol{E}}{\partial t} - \operatorname{curl}\boldsymbol{H} = -\frac{4\pi}{c}\boldsymbol{j}, \quad \operatorname{div}\boldsymbol{E} = 4\pi\rho. \end{aligned} \tag{1}$$

In system (1), $\boldsymbol{E}$ is the electric field, $\boldsymbol{H}$ is the magnetic field, $c$ is the speed of light, and the normalization is chosen so that both the permittivity and permeability of vacuum are equal to one: $\varepsilon_0 = \mu_0 = 1$. System (1) is driven by the extraneous electric charges $\rho = \rho(\boldsymbol{x}, t)$ and currents $\boldsymbol{j} = \boldsymbol{j}(\boldsymbol{x}, t)$, as well as by the magnetic charges $\rho_{\mathrm{m}} = \rho_{\mathrm{m}}(\boldsymbol{x}, t)$ and currents $\boldsymbol{j}_{\mathrm{m}} = \boldsymbol{j}_{\mathrm{m}}(\boldsymbol{x}, t)$. Note that whereas the electric quantities $\rho$ and $\boldsymbol{j}$ have a precise physical meaning, see, e.g. [5], the magnetic quantities $\rho_{\mathrm{m}}$ and $\boldsymbol{j}_{\mathrm{m}}$ in (1) should be interpreted as no more than mathematical artifacts. They are nonexistent in nature and we introduce them in (1) because they will appear in the context of subsequent intermediate derivations; they, however, will never be a part of any final result.

A very important property of system (1) is *the necessary solvability condition* that its right-hand sides (RHSs) must satisfy. By taking divergence of each unsteady equation of (1) and substituting the corresponding steady-state equation we obtain

$$\frac{\partial \rho}{\partial t} + \operatorname{div}\boldsymbol{j} = 0, \tag{2a}$$

$$\frac{\partial \rho_{\mathrm{m}}}{\partial t} + \mathrm{div}\boldsymbol{j}_{\mathrm{m}} = 0. \tag{2b}$$

Eq. (2a) is known as the continuity equation for the electric charges and currents [5]; similarly, Eq. (2b) implies continuity of the artificial magnetic charges and currents. Unless the RHSs of system (1) satisfy relations (2a) and (2b), the Maxwell equations cannot be solved. We will now see what special types of sources may drive the Maxwell system.

The following setup, which is typical for many applications, will be in the center of our subsequent discussion. Assume that there is some possibly complex phenomenon/process confined to a bounded domain $S \subset \mathbb{R}^3$ that manifests itself by the radiation of electromagnetic waves in the far field. As in our previous work [1–3], the domain $S$ is supposed to have a fixed shape, but may move in space according to a prescribed law, so that we will generally have $S = S(t)$, $t > 0$. With no substantial loss of generality, we will restrict ourselves to the case of purely translational motions, which may, though, be unsteady

$$\boldsymbol{u} = \boldsymbol{u}(t), \quad \boldsymbol{U} = \boldsymbol{U}(t) = \int_0^t \boldsymbol{u}(\tau)\,\mathrm{d}\tau \tag{3}$$

here $\boldsymbol{u}$ and $\boldsymbol{U}$ are the vectors of velocity and displacement, respectively, which are the same for every point of $S(t)$. On $\mathbb{R}^3 \setminus S(t)$ the propagation of waves is assumed to be governed by the homogeneous counterpart of the Maxwell system (1). The ultimate objective is to be able to actually solve the problem only on $S(t)$, while truncating all of its exterior and replacing it with special *artificial boundary conditions* (ABCs) at the external boundary $\partial S(t)$.

A key observation that one can make toward fulfilling this objective is to realize that the same wave propagation solution on $\mathbb{R}^3 \setminus S(t)$ as generated by a given radiation mechanism inside $S(t)$ can also be produced by specially chosen divergence-free currents concentrated only on $S(t)$.

**Theorem 1** (Solenoidal currents). *Let the vector fields $\boldsymbol{E} = \boldsymbol{E}(\boldsymbol{x}, t)$ and $\boldsymbol{H} = \boldsymbol{H}(\boldsymbol{x}, t)$ be smooth and satisfy the homogeneous counterpart to Maxwell's system* (1) *on the unbounded region of space–time $\mathbb{R}^3 \setminus S(t) \times [0, +\infty)$, where $S = S(t) \subset \mathbb{R}^3$ is a finite domain with smooth boundary, $\partial S(t) \in C^\infty$. Let also $\boldsymbol{E}(\boldsymbol{x}, 0) = \boldsymbol{H}(\boldsymbol{x}, 0) = \boldsymbol{0}$, $\boldsymbol{x} \in \mathbb{R}^3 \setminus S(0)$. Then, $\exists \tilde{\boldsymbol{j}} = \tilde{\boldsymbol{j}}(\boldsymbol{x}, t)$ and $\tilde{\boldsymbol{j}}_{\mathrm{m}} = \tilde{\boldsymbol{j}}_{\mathrm{m}}(\boldsymbol{x}, t)$:*

- *$\forall t \geqslant 0$ $\{\mathrm{supp}\,\tilde{\boldsymbol{j}}(\boldsymbol{x}, t) \cap \mathbb{R}^3\} \subseteq S(t)$ and $\{\mathrm{supp}\,\tilde{\boldsymbol{j}}_{\mathrm{m}}(\boldsymbol{x}, t) \cap \mathbb{R}^3\} \subseteq S(t)$, i.e., the currents are compactly supported in space for any given moment of time;*
- *$\tilde{\boldsymbol{j}}(\boldsymbol{x}, t)$ and $\tilde{\boldsymbol{j}}_{\mathrm{m}}(\boldsymbol{x}, t)$ are smooth vector fields, and $\mathrm{div}\tilde{\boldsymbol{j}} = 0$ and $\mathrm{div}\tilde{\boldsymbol{j}}_{\mathrm{m}} = 0$;*
- *The solution of system* (1) *on $\mathbb{R}^3$ driven by the currents $\tilde{\boldsymbol{j}}$ and $\tilde{\boldsymbol{j}}_{\mathrm{m}}$ and charges $\tilde{\rho} = \tilde{\rho}_{\mathrm{m}} = 0$ coincides on $\mathbb{R}^3 \setminus S(t)$ with the original $\boldsymbol{E}$ and $\boldsymbol{H}$.*

Note that the homogeneous initial conditions for $\boldsymbol{E}$ and $\boldsymbol{H}$ on $\mathbb{R}^3 \setminus S(0)$ present no loss of generality; they only imply that by the time $t = 0$ no waves have propagated from the domain $S(0)$ outward yet. The RHSs $\tilde{\boldsymbol{j}}$ and $\tilde{\boldsymbol{j}}_{\mathrm{m}}$ that exist according to Theorem 1 will hereafter be referred to as *auxiliary sources*.

**Proof.** To obtain the desired solenoidal currents on $S(t)$, we will first need to represent the quantities $\boldsymbol{H}(\boldsymbol{x}, t)$ and $\boldsymbol{E}(\boldsymbol{x}, t)$ on $\mathbb{R}^3 \setminus S(t)$ as curls of some auxiliary vector fields. Representations of this type are usually constructed in a special convenient form of double curls, as done, for example, when proving the Helmholtz theorem on $\mathbb{R}^3$, see [6, Section 1.5]. For every $t > 0$, let us consider the vector Poisson equation

$$\Delta \boldsymbol{W} = -\boldsymbol{H}, \quad \boldsymbol{x} \in \mathbb{R}^3 \setminus S(t). \tag{4}$$

As the wave propagation speed $c$ is finite, the function $\boldsymbol{H}(\boldsymbol{x}, t)$ will be compactly supported in space for any moment of time $t > 0$. Therefore, we can require that the solution $\boldsymbol{W} = \boldsymbol{W}(\boldsymbol{x}, t)$ of Eq. (4) vanishes at infinity: $\forall t > 0$, $\boldsymbol{W}(\boldsymbol{x}, t) \to 0$ as $|\boldsymbol{x}| \to +\infty$. Next, recasting Eq. (4) in the equivalent form:

$-\operatorname{curl}\operatorname{curl}\boldsymbol{W} + \operatorname{grad}\operatorname{div}\boldsymbol{W} = -\boldsymbol{H}$, and taking divergence of its both sides we obtain that $\operatorname{div}\boldsymbol{W}$ is a harmonic function on $\mathbb{R}^3 \setminus S(t)$

$$\forall t > 0: \qquad \Delta[\operatorname{div}\boldsymbol{W}(\boldsymbol{x},t)] = 0 \quad \text{for } \boldsymbol{x} \in \mathbb{R}^3 \setminus S(t) \tag{5}$$

as $\operatorname{div}\boldsymbol{H} = 0$ on $\mathbb{R}^3 \setminus S(t)$. Note that if Eq. (4) and, consequently, (5), were considered on the entire space $\mathbb{R}^3$, then the Liouville theorem would automatically imply that $\operatorname{div}\boldsymbol{W} \equiv 0$. However, on a domain smaller than the entire space there are many more bounded solutions of (5), and to ensure that the field $\boldsymbol{W}$ be nevertheless divergence-free on $\mathbb{R}^3 \setminus S(t)$, we require that

$$\operatorname{div}\boldsymbol{W}|_{\partial S(t)} = 0. \tag{6}$$

Relation (6) only provides one scalar boundary condition for the vector Poisson equation (4). It still guarantees though that any solution of problem (4), (6) will be solenoidal because Eq. (5) subject to the boundary condition (6) may only have a trivial solution $\operatorname{div}\boldsymbol{W} = 0$ on $\mathbb{R}^3 \setminus S(t)$. Therefore, Eq. (4) reduces to

$$\operatorname{curl}\operatorname{curl}\boldsymbol{W} = \boldsymbol{H}, \quad t > 0, \ \boldsymbol{x} \in \mathbb{R}^3 \setminus S(t) \tag{7}$$

while for $t = 0$ it is natural to set $\boldsymbol{W}(\boldsymbol{x},0) = \boldsymbol{0}$, $\boldsymbol{x} \in \mathbb{R}^3 \setminus S(0)$, as $\boldsymbol{H}(\boldsymbol{x},0) = \boldsymbol{0}$. Our subsequent analysis will make explicit use of the double curl representation for the field $\boldsymbol{H}$ that Eq. (7) offers.

Moreover, we will also need to make sure that the auxiliary field $\boldsymbol{W} = \boldsymbol{W}(\boldsymbol{x},t)$ be a smooth function of all its arguments, including time, even though it is obtained independently for every $t > 0$. Clearly, the regularity in time can only be achieved if one can remove the ambiguity in $\boldsymbol{W}$, which still exists for every $t > 0$ because having only one boundary condition (6) is not sufficient for determining $\boldsymbol{W}$ uniquely. To see what additional boundary conditions at $\partial S(t)$ may be appropriate for Eq. (4) in this perspective, we will first briefly remind of some basic facts pertaining to the volume and surface potentials of the vector Laplacian, while referring the reader to [6, Chapter 13;7, Chapter 3] for detail. The fundamental solution (i.e., free space Green's function) of the operator $\nabla_\beta\nabla^\beta \equiv \Delta$ of (4) [2] is actually a symmetric rank 2 tensor field $\mathfrak{E} = \mathfrak{E}(\boldsymbol{x})$ that solves the following Poisson equation on $\mathbb{R}^3$:

$$\Delta\mathfrak{E} = \mathfrak{g}\delta(\boldsymbol{x}), \tag{8}$$

where $\mathfrak{g}$ is the metric tensor for the coordinates chosen, and $\delta(\boldsymbol{x})$ is the conventional scalar $\delta$-function. As in the Cartesian coordinates the operator in (8) decouples into a set of six conventional scalar Laplacians (six rather than nine, because $\mathfrak{g}$ is symmetric: $g_{\alpha\beta} = g_{\beta\alpha}$), we immediately conclude that

$$\mathfrak{E}(\boldsymbol{x}) = -\frac{1}{4\pi}\frac{\mathfrak{g}(\boldsymbol{x})}{|\boldsymbol{x}|}. \tag{9}$$

Relation (8) implies that if Eq. (4) was to be solved on the entire space $\mathbb{R}^3$ rather than $\mathbb{R}^3 \setminus S(t)$, then its solution would simply be $\boldsymbol{W} = -\mathfrak{E} * \boldsymbol{H}$, where the convolution is assumed to be performed with respect to both the coordinates and the tensor indexes, i.e., $W^\alpha = -\int\int\int_{\mathbb{R}^3} \mathscr{E}^\alpha_\beta(\boldsymbol{x}-\boldsymbol{y})H^\beta(\boldsymbol{y})\,\mathrm{d}\boldsymbol{y}$. Indeed, $\Delta\boldsymbol{W} = -\Delta(\mathfrak{E} * \boldsymbol{H}) = -(\Delta\mathfrak{E}) * \boldsymbol{H} = -(\mathfrak{g}\delta) * \boldsymbol{H} = -\boldsymbol{H}$.

Next, we recall the second Green's formula for the vector quantity $\boldsymbol{W}$ and tensor quantity $\mathfrak{E}$, which reads (see [6, Section 13.1])

[2] Here, $\nabla_\beta$ denotes covariant, and $\nabla^\beta$ denotes contravariant differentiation; unless explicitly specified otherwise, a standard tensor summation with respect to repeated upper and lower indexes is assumed hereafter.

$$\int\int\int_{\mathbb{R}^3\setminus S(t)} \left[\mathfrak{E}(\boldsymbol{x}-\boldsymbol{y})\cdot\Delta\boldsymbol{W}(\boldsymbol{y},t) - \Delta_{\boldsymbol{y}}\mathfrak{E}(\boldsymbol{x}-\boldsymbol{y})\cdot\boldsymbol{W}(\boldsymbol{y},t)\right]\mathrm{d}\boldsymbol{y}$$
$$= \int\int_{\partial S(t)} \left[\mathfrak{E}\times\operatorname{curl}\boldsymbol{W} + \mathfrak{E}\operatorname{div}\boldsymbol{W} - \boldsymbol{W}\times\operatorname{curl}_{\boldsymbol{y}}\mathfrak{E} - \boldsymbol{W}\operatorname{div}_{\boldsymbol{y}}\mathfrak{E}\right]\cdot\boldsymbol{\nu}\,\mathrm{d}S_{\boldsymbol{y}}, \tag{10}$$

where $\boldsymbol{\nu}$ is the unit normal to $\partial S(t)$. The differential operators div and curl applied in formula (10) to the symmetric tensor $\mathfrak{E}$ are defined in a conventional way: $\operatorname{div}\mathfrak{E}^{\alpha} = \nabla_{\beta}\mathscr{E}^{\alpha\beta}$ and $\operatorname{curl}\mathfrak{E}^{\alpha\beta} = \varepsilon^{\alpha\gamma\zeta}\nabla_{\gamma}\mathscr{E}^{\beta}_{\zeta}$, where $\varepsilon^{\alpha\gamma\zeta}$ is the Levi–Civita tensor. Due to the definition of the fundamental solution, see (8), the second term on the left-hand side of Eq. (10) is equal to $-\boldsymbol{W}(\boldsymbol{x},t)$ and we therefore obtain the representation of a vector field as a sum of the volume potential and two surface potentials

$$\boldsymbol{W}(\boldsymbol{x},t) = \int\int\int_{\mathbb{R}^3\setminus S(t)} \underbrace{\mathfrak{E}(\boldsymbol{x}-\boldsymbol{y})\cdot\Delta\boldsymbol{W}(\boldsymbol{y},t)\,\mathrm{d}\boldsymbol{y}}_{\text{volume}}$$
$$+ \int\int_{\partial S(t)} \left[\underbrace{-\mathfrak{E}\times\operatorname{curl}\boldsymbol{W} - \mathfrak{E}\operatorname{div}\boldsymbol{W}}_{\text{single layer}} + \underbrace{\boldsymbol{W}\times\operatorname{curl}_{\boldsymbol{y}}\mathfrak{E} + \boldsymbol{W}\operatorname{div}_{\boldsymbol{y}}\mathfrak{E}}_{\text{double layer}}\right]\cdot\boldsymbol{\nu}\,\mathrm{d}S_{\boldsymbol{y}}. \tag{11}$$

Formula (11) indicates that in addition to the scalar boundary condition (6), one may require, for example, that either the tangential component of $\operatorname{curl}\boldsymbol{W}$ be zero at the boundary (because $[\mathfrak{E}\times\operatorname{curl}\boldsymbol{W}]\cdot\boldsymbol{\nu} = -\mathfrak{E}\cdot[\boldsymbol{\nu}\times\operatorname{curl}\boldsymbol{W}]$)

$$\boldsymbol{\nu}\times\operatorname{curl}\boldsymbol{W}|_{\partial S(t)} = \boldsymbol{0} \tag{12}$$

or the tangential component of the vector $\boldsymbol{W}$ itself be zero at the boundary

$$\boldsymbol{\nu}\times\boldsymbol{W}|_{\partial S(t)} = \boldsymbol{0} \tag{13}$$

(because $[\boldsymbol{W}\times\operatorname{curl}\mathfrak{E}]\cdot\boldsymbol{\nu} = \operatorname{curl}\mathfrak{E}\cdot[\boldsymbol{\nu}\times\boldsymbol{W}]$). Each of the boundary conditions (12) or (13) obviously provides two more scalar constraints for the field $\boldsymbol{W}$ at the surface $\partial S(t)$.

The juxtaposition of boundary conditions (6) and (12) provides a full set of Neumann's boundary conditions for the vector field $\boldsymbol{W}$ at $\partial S(t)$. The juxtaposition of boundary conditions (6) and (13) is a combined Neumann–Dirichlet type boundary condition. Inhomogeneous boundary conditions are also possible, as well as those of the mixed (Robin) type, see [6, Section 13.1].

We, however, are only interested in obtaining a smooth auxiliary field $\boldsymbol{W} = \boldsymbol{W}(\boldsymbol{x},t)$ that would satisfy (4) and (6) but may otherwise be arbitrary. From this standpoint, either of the foregoing choices of boundary conditions will be acceptable. For the combined Neumann–Dirichlet case (6), (13), for example, we can define the Green's function $\mathfrak{G}$ as follows:

$$\mathfrak{G}(\boldsymbol{x},\boldsymbol{y},t) = \mathfrak{E}(\boldsymbol{x}-\boldsymbol{y}) + \mathfrak{F}(\boldsymbol{x},\boldsymbol{y},t), \tag{14a}$$

where $\mathfrak{E}$ is the fundamental solution given by (9) and $\mathfrak{F}$ is a symmetric rank 2 tensor field that satisfies the reciprocity condition

$$\mathfrak{F}(\boldsymbol{x},\boldsymbol{y},t) = \mathfrak{F}(\boldsymbol{y},\boldsymbol{x},t), \quad \boldsymbol{x},\boldsymbol{y}\in\mathbb{R}^3\setminus S(t) \tag{14b}$$

and the Laplace equation

$$\Delta_{\boldsymbol{x}}\mathfrak{F}(\boldsymbol{x},\boldsymbol{y},t) = \boldsymbol{0}, \quad \boldsymbol{x},\boldsymbol{y}\in\mathbb{R}^3\setminus S(t). \tag{14c}$$

The overall Green's function (14a) should also satisfy the boundary conditions

$$\operatorname{div}_{\boldsymbol{x}}\mathfrak{G}|_{\boldsymbol{x}\in\partial S(t)} = \boldsymbol{0}, \quad \boldsymbol{\nu}\times\mathfrak{G}|_{\boldsymbol{x}\in\partial S(t)} = \boldsymbol{0}. \tag{14d}$$

Note, because of the symmetry of all the tensors involved, boundary conditions (14d) provide exactly six independent scalar relations at $\partial S(t)$ for the six independent components of $\mathfrak{F}$. The first three are obviously given by $\operatorname{div}\mathfrak{G}^{\alpha} = \nabla_{\beta}\mathscr{G}^{\beta\alpha} = 0 \Longleftrightarrow \nabla_{\beta}\mathscr{F}^{\beta\alpha} = -\nabla_{\beta}\mathscr{E}^{\beta\alpha}$ for $\alpha = 1,2,3$; and equalities $(\boldsymbol{v}\times\mathfrak{G})^{\alpha\beta} = \varepsilon^{\alpha\gamma\zeta}v_{\gamma}\mathscr{G}^{\beta}_{\zeta} = 0 \Longleftrightarrow \varepsilon^{\alpha\gamma\zeta}v_{\gamma}\mathscr{F}^{\beta}_{\zeta} = -\varepsilon^{\alpha\gamma\zeta}v_{\gamma}\mathscr{E}^{\beta}_{\zeta}$ yield another three. Indeed, assume (with no loss of generality) that the vector $\boldsymbol{v}$ has only one non-zero component $v_{\gamma}$ for some fixed $\gamma$. Then, taking into account that a component of the Levi–Civita tensor may only differ from zero if none of its three indexes is repeated, we conclude that we must have $\mathscr{F}^{\beta}_{\zeta} = -\mathscr{E}^{\beta}_{\zeta}$ for $\beta \neq= \gamma$ and $\zeta \neq= \gamma$, which, along with the symmetry, constitutes three independent scalar relations.

It is also clear that all the unsteadiness in the Green's function (14a) comes only from the boundary conditions (14d) that are set on a moving surface. As, however, these boundary conditions are homogeneous by themselves and do not contain any explicit time dependence, it is easy to conclude that the Green's function (14a) at time $t$ is, in fact, a mere translation of the corresponding Green's function at time $t = 0$:

$$\begin{aligned}\mathfrak{G}(\boldsymbol{x},\boldsymbol{y},t) &= \mathfrak{G}(\boldsymbol{x}-\boldsymbol{U}(t),\boldsymbol{y}-\boldsymbol{U}(t),0)\\ &= \mathfrak{E}(\boldsymbol{x}-\boldsymbol{y}) + \mathfrak{F}^{0}(\boldsymbol{x}-\boldsymbol{U}(t),\boldsymbol{y}-\boldsymbol{U}(t)) \stackrel{\text{def}}{=} \mathfrak{G}^{0}(\boldsymbol{x}-\boldsymbol{U}(t),\boldsymbol{y}-\boldsymbol{U}(t)),\end{aligned} \tag{15}$$

where $\boldsymbol{U}(t)$ is the displacement given by (3).

Having selected the boundary conditions for Eq. (4), and having obtained the corresponding Green's function, we substitute the tensor field $\mathfrak{F}(\boldsymbol{x},y,t) = \mathfrak{F}^{0}(\boldsymbol{x}-\boldsymbol{U}(t),\boldsymbol{y}-\boldsymbol{U}(t))$ of (14a), (15) into formula (10) instead of the fundamental solution $\mathfrak{E}$ and use the reciprocity condition (14b) along with the property (14c), which altogether yields:

$$\begin{aligned}\boldsymbol{0} = &\int\int\int_{\mathbb{R}^3\setminus S(t)} \mathfrak{F}^{0}(\boldsymbol{x}-\boldsymbol{U}(t),\boldsymbol{y}-\boldsymbol{U}(t))\cdot\Delta\boldsymbol{W}(\boldsymbol{y},t)\,\mathrm{d}\boldsymbol{y}\\ &+\int\int_{\partial S(t)}\left[-\mathfrak{F}\times\operatorname{curl}\boldsymbol{W} - \mathfrak{F}\operatorname{div}\boldsymbol{W} + \boldsymbol{W}\times\operatorname{curl}_{y}\mathfrak{F} + \boldsymbol{W}\operatorname{div}_{y}\mathfrak{F}\right]\cdot\boldsymbol{v}\,\mathrm{d}S_{y}.\end{aligned} \tag{16}$$

Next, by adding Eqs. (11) and (16) and using conditions (14d) we obtain

$$\begin{aligned}\boldsymbol{W}(\boldsymbol{x},t) = &\int\int\int_{\mathbb{R}^3\setminus S(t)} \mathfrak{G}^{0}(\boldsymbol{x}-\boldsymbol{U}(t),\boldsymbol{y}-\boldsymbol{U}(t))\cdot\Delta\boldsymbol{W}(\boldsymbol{y},t)\,\mathrm{d}\boldsymbol{y}\\ &+\int\int_{\partial S(t)}\left[-\mathfrak{G}\cdot\boldsymbol{v}\ \operatorname{div}\boldsymbol{W} + \operatorname{curl}_{y}\mathfrak{G}\cdot(\boldsymbol{v}\times\boldsymbol{W})\right]\mathrm{d}S_{y}.\end{aligned} \tag{17}$$

Finally, we substitute the homogeneous boundary values from (6) and (13) into the surface integrals on the right-hand side of (17), then substitute $\boldsymbol{H}(\boldsymbol{y},t) = -\Delta\boldsymbol{W}(\boldsymbol{y},t)$ into the corresponding volume integral, and obtain

$$\boldsymbol{W}(\boldsymbol{x},t) = -\int\int\int_{\mathbb{R}^3\setminus S(t)} \mathfrak{G}^{0}(\boldsymbol{x}-\boldsymbol{U}(t),\boldsymbol{y}-\boldsymbol{U}(t))\cdot\boldsymbol{H}(\boldsymbol{y},t)\,\mathrm{d}\boldsymbol{y}. \tag{18}$$

Formula (18) is the Green's function representation of the solution $\boldsymbol{W}(\boldsymbol{x},t)$ to the boundary-value problem (4), (6), (13). It will help us establish the required smoothness of $\boldsymbol{W}(\boldsymbol{x},t)$ with respect to all its arguments, provided that the source term $\boldsymbol{H}(\boldsymbol{x},t)$ is also smooth. In so doing, it is clear that only the regularity in time may require a special comment, whereas the regularity of $\boldsymbol{W}(\boldsymbol{x},t)$ in space would follow from the standard elliptic considerations.

The region of integration $\mathbb{R}^3 \setminus S(t)$ in formula (18) is obviously not stationary. Therefore, for future convenience, let us introduce a new vector field

$$\hat{\boldsymbol{H}}(\boldsymbol{y},t) \stackrel{\text{def}}{=} \boldsymbol{H}(\boldsymbol{y}+\boldsymbol{U}(\mathrm{t}),\mathrm{t}) \tag{19}$$

which would allow us to recast formula (18) so that the integration be now performed over a fixed domain $\mathbb{R}^3 \setminus S(0)$

$$\begin{aligned}\boldsymbol{W}(\boldsymbol{x},t) &= -\int\int\int_{\mathbb{R}^3\setminus S(t)} \mathfrak{G}^0(\boldsymbol{x}-\boldsymbol{U}(t),\boldsymbol{y}-\boldsymbol{U}(t))\cdot\hat{\boldsymbol{H}}(\boldsymbol{y}-\boldsymbol{U}(t),t)\,\mathrm{d}\boldsymbol{y}\\ &= -\int\int\int_{\mathbb{R}^3\setminus S(0)} \mathfrak{G}^0(\boldsymbol{x}-\boldsymbol{U}(t),\boldsymbol{y}')\cdot\hat{\boldsymbol{H}}(\boldsymbol{y}',t)\,\mathrm{d}\boldsymbol{y}'.\end{aligned} \tag{20}$$

Differentiating (20) with respect to time, we obtain

$$\begin{aligned}\frac{\partial\boldsymbol{W}(\boldsymbol{x},t)}{\partial t} &= \int\int\int_{\mathbb{R}^3\setminus S(0)} \Big[\boldsymbol{u}(t)\cdot\operatorname{grad}_{\boldsymbol{x}}\mathfrak{G}^0(\boldsymbol{x}-\boldsymbol{U}(t),\boldsymbol{y}')\Big]\cdot\hat{\boldsymbol{H}}(\boldsymbol{y}',t)\,\mathrm{d}\boldsymbol{y}'\\ &\quad -\int\int\int_{\mathbb{R}^3\setminus S(0)} \mathfrak{G}^0(\boldsymbol{x}-\boldsymbol{U}(t),\boldsymbol{y}')\cdot\frac{\partial\hat{\boldsymbol{H}}(\boldsymbol{y}',t)}{\partial t}\,\mathrm{d}\boldsymbol{y}'.\end{aligned} \tag{21}$$

The first term on the right-hand side of (21) is equal to $-\boldsymbol{u}(t)\cdot\operatorname{grad}\boldsymbol{W}(\boldsymbol{x},t)$ and is continuous. The second term contains the partial derivative of $\hat{\boldsymbol{H}}$ with respect to time, which, according to (19), shall be expressed as $\frac{\partial\hat{\boldsymbol{H}}(\boldsymbol{y}',t)}{\partial t} = \boldsymbol{u}(t)\cdot\operatorname{grad}\boldsymbol{H}(\boldsymbol{y}'+\boldsymbol{U}(t),t) + \frac{\partial\boldsymbol{H}(\boldsymbol{y}'+\boldsymbol{U}(t),t)}{\partial t}$; it is, as such, continuous, provided that the corresponding derivatives of $\boldsymbol{H}$ are continuous. Existence and continuity of the higher-order derivatives of $\boldsymbol{W}(\boldsymbol{x},t)$ w.r.t. time can be established similarly, by further differentiating (21). They will obviously hinge on the regularity of $\boldsymbol{H}(\boldsymbol{y},t)$ and on that of the law of motion (3).

Altogether, we have been able to construct a smooth auxiliary vector field $\boldsymbol{W} = \boldsymbol{W}(\boldsymbol{x},t)$ on $\mathbb{R}^3 \setminus S(t)$ for all $t > 0$, such that the given magnetic field $\boldsymbol{H} = \boldsymbol{H}(\boldsymbol{x},t)$, $\operatorname{div}\boldsymbol{H} = 0$, is represented in the double curl form (7). Quite similarly, considering the problem

$$\Delta\boldsymbol{V} = -\boldsymbol{E}, \quad \boldsymbol{x}\in\mathbb{R}^3\setminus S(t), \tag{22a}$$

$$\operatorname{div}\boldsymbol{V}|_{\partial S(t)} = 0, \tag{22b}$$

$$\boldsymbol{v}\times\boldsymbol{V}|_{\partial S(t)} = \boldsymbol{0}, \tag{22c}$$

we arrive at the following representation for the electric field [cf. (7)]:

$$\operatorname{curl}\operatorname{curl}\boldsymbol{V} = \boldsymbol{E}, \quad t>0,\ \boldsymbol{x}\in\mathbb{R}^3\setminus S(t), \tag{23}$$

where, again, $\boldsymbol{V}(\boldsymbol{x},0) = \boldsymbol{0}$, $\boldsymbol{x}\in\mathbb{R}^3\setminus S(0)$, because $\boldsymbol{E}(\boldsymbol{x},0) = \boldsymbol{0}$.

For the last phase of the proof, we will use an extension argument of Whitney's type that applies to functions defined on closed sets, see [8, Chapter VI]. Let $\varepsilon > 0$ and introduce a smaller sub-domain $S_\varepsilon = S_\varepsilon(t) \stackrel{\text{def}}{=} \{\boldsymbol{x}\in\mathrm{S(t)}\,|\,\operatorname{dist}(\boldsymbol{x},\partial\mathrm{S(t)}) > \varepsilon\}$. Hereafter, we will call $S(t)\setminus S_\varepsilon(t)$ the transition region, see Fig. 1. The previously built auxiliary vector field $\boldsymbol{W} = \boldsymbol{W}(\boldsymbol{x},t)$ can be extended inwards from its four-dimensional space–time domain $\mathbb{R}^3\setminus S(t)$, $t>0$ [$S(t)$ is assumed an open set, therefore, $\mathbb{R}^3\setminus S(t)$ is a closed set] to this transition region for $t>0$; the extension $\tilde{\boldsymbol{W}} = \tilde{\boldsymbol{W}}(\boldsymbol{x},t)$ will be defined on a larger domain $\mathbb{R}^3\setminus S_\varepsilon(t)$, $t>0$, and will still coincide with $\boldsymbol{W}$ on $\mathbb{R}^3\setminus S(t)$, $t>0$. For $t=0$, obviously, $\tilde{\boldsymbol{W}}(\boldsymbol{x},0) = \boldsymbol{0}$, $\boldsymbol{x}\in\mathbb{R}^3\setminus S_\varepsilon(0)$. Moreover, since the boundary is assumed smooth, $\partial S(t)\in C^\infty$, the extension $\tilde{\boldsymbol{W}}(\boldsymbol{x},t)$ can be obtained so

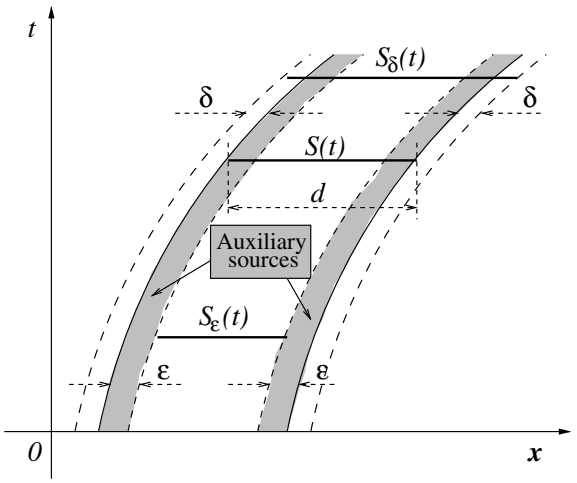


Fig. 1. Schematic geometry.

that it would have as many continuous derivatives (w.r.t. all its arguments) on $\mathbb{R}^3 \setminus S_\varepsilon(t)$, $t > 0$, as $\boldsymbol{W}(\boldsymbol{x}, t)$ has on $\mathbb{R}^3 \setminus S(t)$, $t > 0$; these derivatives of $\tilde{\boldsymbol{W}}$ will be uniformly bounded [i.e., independently of $(\boldsymbol{x}, t)$] in terms of the corresponding derivatives of $\boldsymbol{W}$. Of course, an extension $\tilde{\boldsymbol{V}}$ that would have the same properties can be built for the auxiliary field $\boldsymbol{V}$ of (22a)–(22c). Clearly, none of these extensions is unique. We, however, only need their existence.

Let now $\mu = \mu(\boldsymbol{x}, t)$ be a smooth scalar multiplier function:

$$\forall t > 0: \qquad \mu(\boldsymbol{x}, t) = \begin{cases} 0, & \boldsymbol{x} \in S_\varepsilon(t), \\ 1, & \boldsymbol{x} \in \mathbb{R}^3 \setminus S(t), \\ \in (0,1), & \boldsymbol{x} \in S(t) \setminus S_\varepsilon(t) \end{cases} \tag{24}$$

and apply it to $\tilde{\boldsymbol{V}}$ and $\tilde{\boldsymbol{W}}$, i.e., obtain $\mu\tilde{\boldsymbol{V}}$ and $\mu\tilde{\boldsymbol{W}}$. Even though we did not require that $\tilde{\boldsymbol{V}}(\boldsymbol{x}, t)$ and $\tilde{\boldsymbol{W}}(\boldsymbol{x}, t)$ be defined further inwards beyond the transition region $S(t) \setminus S_\varepsilon(t)$, one can obviously consider the functions $\mu\tilde{\boldsymbol{V}}$ and $\mu\tilde{\boldsymbol{W}}$ on the entire space $\mathbb{R}^3$ for any $t > 0$, because $\mu = 0$ for $\boldsymbol{x} \in S_\varepsilon(t)$ anyway. On $\mathbb{R}^3 \setminus S(t)$, these functions coincide with $\boldsymbol{V}$ and $\boldsymbol{W}$, respectively; and on $S(t) \setminus S_\varepsilon(t)$, they undergo a smooth transition from their far-field values [i.e., values on $\mathbb{R}^3 \setminus S(t)$] to zero. For $t = 0$, $\mu\tilde{\boldsymbol{V}} = \mu\tilde{\boldsymbol{W}} = \boldsymbol{0}$, $\boldsymbol{x} \in \mathbb{R}^3$. Next, define

$$\tilde{\boldsymbol{E}} = \operatorname{curl}\operatorname{curl}(\mu\tilde{\boldsymbol{V}}), \quad \tilde{\boldsymbol{H}} = \operatorname{curl}\operatorname{curl}(\mu\tilde{\boldsymbol{W}}), \quad t > 0, \ \boldsymbol{x} \in \mathbb{R}^3. \tag{25}$$

The modified quantities $\tilde{\boldsymbol{E}}$ and $\tilde{\boldsymbol{H}}$ of (25) coincide with the original quantities $\boldsymbol{E}$ and $\boldsymbol{H}$, respectively, in the far field, i.e., on $\mathbb{R}^3 \setminus S(t)$, $t > 0$; they are both equal to zero on $S_\varepsilon(t)$ because of (24); and on $S(t) \setminus S_\varepsilon(t)$, $t > 0$, they, again, undergo a smooth transition from their far-field values to zero. For $t = 0$, we obtain $\tilde{\boldsymbol{E}}(\boldsymbol{x}, 0) = \tilde{\boldsymbol{H}}(\boldsymbol{x}, 0) = \boldsymbol{0}$, $\boldsymbol{x} \in \mathbb{R}^3$, which is an extension of the homogeneous far-field initial conditions into $S(0)$.

The key reason for obtaining extensions for the electric and magnetic fields in the specific double curl form (25) is that while being smooth across the entire space, the new fields $\tilde{\boldsymbol{E}}$ and $\tilde{\boldsymbol{H}}$ obviously satisfy

$$\operatorname{div}\tilde{\boldsymbol{E}} = \operatorname{div}\tilde{\boldsymbol{H}} \equiv 0, \quad t > 0, \ \boldsymbol{x} \in \mathbb{R}^3. \tag{26}$$

Then, the required auxiliary RHSs $\tilde{\boldsymbol{j}}, \tilde{\boldsymbol{j}}_{\mathrm{m}}, \tilde{\rho}$, and $\tilde{\rho}_{\mathrm{m}}$ are constructed by substituting the modified fields $\tilde{\boldsymbol{E}}$ and $\tilde{\boldsymbol{H}}$ of (25) into the left-hand sides of Eq. (1) on the entire space $\mathbb{R}^3$. In so doing, relations (26) immediately

imply that the resulting auxiliary charges will be trivial: $\tilde{\rho} = \tilde{\rho}_{\mathrm{m}} = 0$, while the corresponding auxiliary currents will appear solenoidal, $\mathrm{div}\tilde{\boldsymbol{j}} = \mathrm{div}\tilde{\boldsymbol{j}}_{\mathrm{m}} = 0$. The latter can be shown directly by taking divergence of each unsteady equation (1) and using equalities (26) again.

The RHSs $\tilde{\boldsymbol{j}}$ and $\tilde{\boldsymbol{j}}_{\mathrm{m}}$ obtained this way will be sufficiently smooth everywhere, because of the smoothness of Whitney's extensions, and that of the multiplier $\mu$ of (24). Moreover, they may only differ from zero on $S(t) \setminus S_{\varepsilon}(t)$, because on $S_{\varepsilon}(t)\tilde{\boldsymbol{E}} = \tilde{\boldsymbol{H}} = \boldsymbol{0}$, and on $\mathbb{R}^3 \setminus S(t)$ $\tilde{\boldsymbol{E}} = \boldsymbol{E}$, $\tilde{\boldsymbol{H}} = \boldsymbol{H}$, for which the homogeneous Maxwell equations hold. In other words, $\forall t > 0 : \{\mathrm{supp}\tilde{\boldsymbol{j}}(\boldsymbol{x}, t) \cap \mathbb{R}^3\} \subseteq S(t) \setminus S_{\varepsilon}(t)$ and $\{\mathrm{supp}\tilde{\boldsymbol{j}}_{\mathrm{m}}(\boldsymbol{x}, t) \cap \mathbb{R}^3\} \subseteq S(t) \setminus S_{\varepsilon}(t)$, which is an even stronger statement than originally formulated in the theorem.

Solution of the Maxwell system (1) driven by the auxiliary sources $\tilde{\boldsymbol{j}}$, $\tilde{\boldsymbol{j}}_{\mathrm{m}}$, $\tilde{\rho} = 0$, and $\tilde{\rho}_{\mathrm{m}} = 0$, with homogeneous initial conditions, is equal to $\tilde{\boldsymbol{E}}(\boldsymbol{x}, t)$, $\tilde{\boldsymbol{H}}(\boldsymbol{x}, t)$ for $\boldsymbol{x} \in \mathbb{R}^3$ and $t \geqslant 0$ due to the uniqueness. Consequently, it coincides with $\boldsymbol{E}(\boldsymbol{x}, t)$, $\boldsymbol{H}(\boldsymbol{x}, t)$ on $\mathbb{R}^3 \setminus S(t) \times [0, +\infty)$, as required. □

**Corollary 2** (A basis for numerics). *The quantities* $\tilde{\boldsymbol{j}}$, $\tilde{\boldsymbol{j}}_{\mathrm{m}}$, $\tilde{\rho}$, *and* $\tilde{\rho}_{\mathrm{m}}$ *of Theorem* 1 *satisfy Eqs.* (2a) *and* (2b) *identically* $\forall t \geqslant 0$ *and* $\boldsymbol{x} \in \mathbb{R}^3$.

**Corollary 3.** *To obtain the solenoidal currents* $\tilde{\boldsymbol{j}} = \tilde{\boldsymbol{j}}(\boldsymbol{x}, t)$ *and* $\tilde{\boldsymbol{j}}_{\mathrm{m}} = \tilde{\boldsymbol{j}}_{\mathrm{m}}(\boldsymbol{x}, t)$ *that exist according to Theorem* 1, *it is, in fact, sufficient to know the fields* $\boldsymbol{H} = \boldsymbol{H}_S(\boldsymbol{x}, t)$ *and* $\boldsymbol{E} = \boldsymbol{E}_S(\boldsymbol{x}, t)$ *only at the boundary* $\partial S(t)$ *for* $t > 0$.

**Proof.** The electric and magnetic fields on $\mathbb{R}^3 \setminus S(t)$, $t > 0$, are governed by the homogeneous Maxwell equations. Taking curl of one unsteady equation from the homogeneous counterpart of system (1), differentiating the remaining unsteady equation with respect to time, substituting into one another, and using the identity $\mathrm{curl}\,\mathrm{curl}[\cdots] = -\Delta[\cdots] + \mathrm{grad}\,\mathrm{div}[\cdots]$ along with the corresponding steady-state equation, we arrive at the following individual equations for the fields:

$$\frac{1}{c^2}\frac{\partial^2 \boldsymbol{H}}{\partial t^2} - \Delta \boldsymbol{H} = \boldsymbol{0}, \quad \frac{1}{c^2}\frac{\partial^2 \boldsymbol{E}}{\partial t^2} - \Delta \boldsymbol{E} = \boldsymbol{0}. \tag{27}$$

In other words, every solution to the homogeneous Maxwell equations on $\mathbb{R}^3 \setminus S(t)$, $t > 0$, is also a solution to the homogeneous vector wave Eq. (27). Eqs. (27) need to be supplemented by the homogeneous initial conditions $\boldsymbol{H}(\boldsymbol{x}, 0) = \boldsymbol{E}(\boldsymbol{x}, 0) = \boldsymbol{0}$, $\boldsymbol{x} \in \mathbb{R}^n \setminus S(0)$ (cf. Theorem 1) and by the Dirichlet conditions

$$\forall t > 0 : \qquad \boldsymbol{H}(\boldsymbol{x}, t)|_{\boldsymbol{x} \in S(t)} = \boldsymbol{H}_S(\boldsymbol{x}, t), \quad \boldsymbol{E}(\boldsymbol{x}, t)|_{\boldsymbol{x} \in S(t)} = \boldsymbol{E}_S(\boldsymbol{x}, t) \tag{28}$$

at the lateral boundary $\partial S(t)$. Under the natural assumption that the maximum speed of motion in (3) is always smaller than the characteristic speed, $\max_t |\boldsymbol{u}(t)| < c$, we conclude that problems (27) and (28) are uniquely solvable and consequently, the fields $\boldsymbol{H} = \boldsymbol{H}(\boldsymbol{x}, t)$ and $\boldsymbol{E} = \boldsymbol{E}(\boldsymbol{x}, t)$ can be unambiguously reconstructed on $\mathbb{R}^3 \setminus S(t)$, $t > 0$, from their boundary data $\boldsymbol{H}_S(\boldsymbol{x}, t)$ and $\boldsymbol{E}_S(\boldsymbol{x}, t)$, respectively. Then, Theorem 1 yields the required $\tilde{\boldsymbol{j}}$ and $\tilde{\boldsymbol{j}}_{\mathrm{m}}$. □

A few essential comments are now in order. First and foremost, smoothness of the Whitney extensions $\tilde{\boldsymbol{V}}$ and $\tilde{\boldsymbol{W}}$, as well as that of the multiplier $\mu$ of (24), is of key importance. Otherwise, differentiation in (25), as well as differentiation of $\tilde{\boldsymbol{E}}$ and $\tilde{\boldsymbol{H}}$ when substituted into the left-hand sides of the Maxwell system (1), may generate singularities along the interface $\partial S(t)$.

Besides, recall that the electromagnetic field is determined by its vector and scalar potentials that usually satisfy a particular gauge. Under the Coulomb gauge the scalar potential is identically equal to zero. On the region where no sources are present, such as $\mathbb{R}^3 \setminus S(t)$, one can additionally require that the vector potential $\boldsymbol{A}$ be solenoidal, see [5, Chapters III and VI], which yields

$$\boldsymbol{H} = \mathrm{curl}\,\boldsymbol{A}, \quad \boldsymbol{E} = -\frac{1}{c}\frac{\partial \boldsymbol{A}}{\partial t}, \quad \mathrm{div}\,\boldsymbol{A} = 0. \tag{29}$$

By looking at the first and third equations of (29) we conclude that if we new the particular auxiliary field $\boldsymbol{W}_A = \boldsymbol{W}_A(\boldsymbol{x},t)$ that generates the true physical vector potential: $\boldsymbol{A} = \boldsymbol{A}(\boldsymbol{x},t) = \operatorname{curl} \boldsymbol{W}_A(\boldsymbol{x},t)$, then we could have used it when constructing the solenoidal auxiliary currents in the concluding part of the proof of Theorem 1. In so doing, we would have defined the modified magnetic field as before: $\tilde{\boldsymbol{H}} = \operatorname{curl}\operatorname{curl}(\mu\tilde{\boldsymbol{W}}_A)$, cf. formulae (25). As concerns the modified electric field, we would have rather defined it in accordance with (29): $\tilde{\boldsymbol{E}} = -\frac{1}{c}\frac{\partial}{\partial t}\operatorname{curl}(\mu\tilde{\boldsymbol{W}}_A)$, thus bypassing the entire part of the derivation that involves the second auxiliary quantity $\boldsymbol{V} = \boldsymbol{V}(\boldsymbol{x},t)$, see (22a)–(22c). An easy verification shows that this approach would still yield the solenoidal auxiliary currents and zero auxiliary charges on $S(t) \setminus S_\varepsilon(t)$, see Fig. 1. Moreover, in this case the magnetic currents would be identically equal to zero: $\tilde{\boldsymbol{j}}_{\mathrm{m}}(\boldsymbol{x},t) \equiv \boldsymbol{0}$, which corresponds to the genuine physics, and which should clearly be expected when using the Coulomb gauge (29).

In general, however, the vector potential $\boldsymbol{A}$ of (29) and the field $\operatorname{curl} \boldsymbol{W}$ of (7) are not the same; they may differ by the gradient of a harmonic function $\varphi(\boldsymbol{x},t)$, $\Delta\varphi = 0$. When proving Theorem 1, we have employed boundary conditions (6) and (13) to specify $\boldsymbol{W} = \boldsymbol{W}(\boldsymbol{x},t)$ on $\mathbb{R}^3 \setminus S(t)$ uniquely. Even though many other boundary conditions can be set at $\partial S(t)$ that would lead to a unique solution of the Poisson equation (4), selection of those that would guarantee $\operatorname{curl} \boldsymbol{W} = \boldsymbol{A}$ is by no means an obvious task. In general, this is a key difficulty in using the actual physical vector potential $\boldsymbol{A}$ of (29) as a vehicle for obtaining the solenoidal auxiliary currents. On the other hand, the proof of Theorem 1 that involves independent extensions for $\boldsymbol{H}$ and $\boldsymbol{E}$ (via $\tilde{\boldsymbol{W}}$ and $\tilde{\boldsymbol{V}}$) provides a substantially more straightforward venue toward divergence-free $\tilde{\boldsymbol{j}}$ and $\tilde{\boldsymbol{j}}_{\mathrm{m}}$, even though it does produce a non-trivial $\tilde{\boldsymbol{j}}_{\mathrm{m}}(\boldsymbol{x},t)$. This, in particular, demonstrates the importance of allowing for the non-physical magnetic currents (and charges) on the RHS of (1) ahead of time.

We should emphasize, though, that there may still be special situations when the vector potential $\boldsymbol{A}$ of (29) can be exploited. One of those is the so-called transverse magnetic mode with cylindrical symmetry. It is analyzed in Section 5 of the paper, in which a simplified argument is developed that substitutes for the proof of Theorem 1. The computations of Section 5 clearly demonstrate that the use of the solenoidal auxiliary currents completely eliminates all the obstacles in implementation of the lacunae-based ABCs for the Maxwell equations. This observation experimentally corroborates the central role of Theorem 1 as a theoretical result that guarantees existence of the critical algorithm components.

On the other hand, we also need to mention that in general the proof of Theorem 1 itself does not provide a constructive procedure for obtaining the solenoidal auxiliary currents, because it requires solving additional boundary-value problems (4), (6), (13) and (22a)–(22c). Theorem 1 shall rather be regarded as a fundamental existence statement, whereas in a practical computational setting solution of problems (4), (6), (13) and (22a)–(22c) must be replaced by a more efficient alternative. As has been mentioned, one such alternative, which only works for a particular formulation, is based on the use of the vector potential $\boldsymbol{A}$, see Section 5. A substantially more general alternative of this type has also been developed; it is based on obtaining the extended auxiliary fields $\tilde{\boldsymbol{W}}$ and $\tilde{\boldsymbol{V}}$ in the form of special Taylor expansions, which only employ the boundary data for $\boldsymbol{H}$ and $\boldsymbol{E}$, as prescribed by Corollary 3. The corresponding algorithm does not require solving any additional PDEs; at the same time it is not restricted to only particular cases either. This Taylor-based approach will be reported on in our future paper [4].

From the general theoretical standpoint, Theorem 1 introduces a conclusive formulation and establishes solvability of a class of time-dependent inverse problems for electromagnetic fields. It will therefore be instrumental to assess the meaning and significance of this result in the framework of the inverse scattering theory. An inverse scattering problem per se usually consists of reconstructing the shape of the scatterer once the scattered electromagnetic field is known (or at least some data about this field are available). Neither in the time domain, nor in the frequency domain (see, e.g. [9,10]) is its solution unique. A conceptually more close formulation is known as the inverse source problem that can also be studied in the time domain, as well as in the frequency domain. It consists of reconstructing the sources of the electromagnetic field (currents and charges on the right-hand side of the governing equations) once the field itself is known. Solution to this problem is not unique either,

see, e.g. [10] for the frequency domain analysis. In the time domain, the inverse source formulation [11] requires finding the currents and charges that operated in the past and that generate the field specified at the present moment of time. Even though this problem has multiple solutions, Moses [11] and Moses and Prosser [12] have shown that it still allows one to identify special uniqueness classes for the inverse sources that satisfy the appropriately chosen additional conditions. In contradistinction to these classical problems, in the genuinely unsteady formulation of Theorem 1, we use the information about the field not at some given moment of time, but on the entire interval of interest. On the other hand, the auxiliary sources that we want to reconstruct must satisfy rather strict constraints; namely, the currents must be smooth, have compact support, and be solenoidal. Nonetheless, as proof of Theorem 1 indicates, this problem has many solutions as well [various choices for $\boldsymbol{W}$ and $\boldsymbol{V}$ in the first place, many different ways of obtaining the extensions $\tilde{\boldsymbol{W}}$ and $\tilde{\boldsymbol{V}}$, and many choices for the multiplier $\mu$ of (24)]. Perhaps the closest formulation analyzed previously in the literature is that by Devaney and Wolf [13]. In this work, the authors introduce and study the notion of the so-called non-radiating currents in the frequency domain. The latter are compactly supported currents that are supposed to generate no field outside a predetermined region of space. Theorem IV of paper [13] states that any such current distribution can be obtained by applying essentially the vector Helmholtz operator to the auxiliary (electric) field that vanishes outside the aforementioned region. As such, Theorem 1 can be thought of as an extension of the latter result to the time domain case with both fields $\boldsymbol{E}$ and $\boldsymbol{H}$ present, when the currents are supposed to generate a particular radiation pattern instead of simply being non-radiating, and are also supposed to satisfy some additional conditions (be solenoidal).

## 3. The auxiliary problem and its integration using lacunae

Let the Maxwell system (1) be driven by the solenoidal currents and zero charges that exist according to Theorem 1. Once considered on the entire space $\mathbb{R}^3$ subject to the homogeneous initial conditions, this system will be referred to as *the auxiliary problem*. The auxiliary problem is, of course, not completely independent. In the following Section 4 it will appear as a part of decomposition of the original problem needed for setting the ABCs on $\partial S(t)$. In the meantime, though, we will assume that the source terms $\tilde{\boldsymbol{j}}(\boldsymbol{x},t)$ and $\tilde{\boldsymbol{j}}_{\mathrm{m}}(\boldsymbol{x},t)$ are simply given for $\boldsymbol{x}\in S(t)\setminus S_{\varepsilon}(t)$ and $t>0$, and describe the solution methodology for the auxiliary problem. This methodology will be based on the special property of the Maxwell equations known as the presence of *lacunae* in their solutions. We will see that it enables a very efficient long-term numerical integration procedure. However, it is not attainable routinely unless the continuity equations for the RHSs (2a) and (2b) are satisfied identically – the property guaranteed by Corollary 2 provided that the conditions of Theorem 1 hold.

We will first analyze the general case, with no special reference to the solenoidal currents. The same argument as employed when proving Corollary 3, only applied to the full inhomogeneous system (1), yields the inhomogeneous vector wave equations for the fields $\boldsymbol{H}=\boldsymbol{H}(\boldsymbol{x},t)$ and $\boldsymbol{E}=\boldsymbol{E}(\boldsymbol{x},t)$:

$$\begin{aligned}
&\frac{1}{c^2}\frac{\partial^2\boldsymbol{H}}{\partial t^2}-\Delta\boldsymbol{H}=-4\pi\left[\frac{1}{c^2}\frac{\partial\boldsymbol{j}_{\mathrm{m}}}{\partial t}-\frac{1}{c}\operatorname{curl}\boldsymbol{j}+\operatorname{grad}\rho_{\mathrm{m}}\right],\\
&\frac{1}{c^2}\frac{\partial^2\boldsymbol{E}}{\partial t^2}-\Delta\boldsymbol{E}=-4\pi\left[\frac{1}{c^2}\frac{\partial\boldsymbol{j}}{\partial t}+\frac{1}{c}\operatorname{curl}\boldsymbol{j}_{\mathrm{m}}+\operatorname{grad}\rho\right].
\end{aligned}\tag{30}$$

If the currents and charges in system (1) were *compactly supported in space and time* on some domain $Q\subset\mathbb{R}^3\times[0,+\infty)$, then the RHSs in Eq. (30) would be compactly supported on the same domain $Q$ as well, and the solutions $\boldsymbol{E}=\boldsymbol{E}(\boldsymbol{x},t)$ and $\boldsymbol{H}=\boldsymbol{H}(\boldsymbol{x},t)$ *would have lacunae* [14]:

$$\boldsymbol{E} = \boldsymbol{H} \equiv 0 \quad \forall (\boldsymbol{x}, t) \in \bigcap_{(\boldsymbol{\xi},\tau)\in Q} \{(\boldsymbol{x}, t) || \boldsymbol{x} - \boldsymbol{\xi}| < c(t-\tau),\ t > \tau\}. \tag{31}$$

Lacuna of the solution (31) is obtained as the intersection of all characteristic cones (light cones) of a given wave equation (30) once the vertex of the cone sweeps the support of the corresponding right-hand side. From the standpoint of physics, lacuna is the part of space–time, on which the waves generated by a compactly supported source have already passed, and the solution has become zero again. The phenomenon of lacunae is inherently three-dimensional. The surface of the lacuna represents the trajectory of aft (trailing) fronts of the waves. The existence of *sharp aft fronts* in odd-dimension spaces is known as the Huygens' principle, as opposed to the so-called wave diffusion, which takes place in even-dimension spaces, see, e.g. [15,16].

Let us note that the question of classifying those hyperbolic equations and systems that admit the diffusionless propagation of waves has first been formulated in the literature by Hadamard [17–19]. He himself did not know any other examples besides the classical wave (d'Alembert) equation. The notion of lacunae was introduced and studied by Petrowsky in work [14], see also [16, Chapter VI]. He, in particular, has obtained general conditions for the coefficients of hyperbolic equations that guaranteed existence of lacunae. Subsequently, the ideas of Petrowsky have been further developed by Atiyah et al. [20,21]. However, since work [14] no other constructive examples of either scalar equations or systems have been found that would have lacunae in their solutions, except the wave equation and its equivalents. More precisely, Matthisson [22] has shown that in the standard $(3+1)$-dimensional space–time with the Minkowski metric the only scalar hyperbolic equation that satisfies the Huygens' principle is the wave equation. Later, Stellmacher [23–25] has built examples of nontrivial (i.e., irreducible to the wave equation) diffusionless equations, but only in the spaces $\mathbb{R}^n$ for odd $n \geqslant 5$. There are also examples of nontrivial diffusionless (i.e., Huygens') systems (as opposed to scalar equations) in the standard Minkowski $3+1$ space–time [26–28], and examples of nontrivial scalar Huygens' equations in a $(3+1)$-dimensional space–time but equipped with an alternative (the so-called plane wave) metric, see [27–29].

The presence of lacunae suggests a very natural way of integrating system (1) driven by compactly supported sources. Let $Q = \{(\boldsymbol{x}, t) | \boldsymbol{x} \in S(t), t_0 < t < t_1\}$, and assume that we need to know the solution on a larger (but still finite) domain $S_\delta(t)$, see Fig. 1. It is easy to show [1–3] that by the time

$$t_2 = t_0 + \frac{d + 2\delta + (t_1 - t_0)(c+k)}{c-k} \equiv t_0 + T_{\text{int}} \tag{32}$$

the domain $S_\delta(t)$ will completely fall into the lacuna (31) and will remain inside the lacuna continuously thereafter, i.e., $\forall t \geqslant t_2$. In formula (32), $d \stackrel{\text{def}}{=} \text{diamS(t)}$ so that $d + 2\delta = \text{diam}S_\delta(t)$, and $k = \max_t |\boldsymbol{u}(t)|$, $k < c$, is the maximum speed of motion for the domain $S(t)$, see formula (3). Consequently, we can employ any appropriate numerical method (say, a consistent and stable finite-difference scheme) to integrate system (1) on the finite interval $T_{\text{int}}$. After the time $T_{\text{int}}$ elapses since the the inception of the sources $t_0$, we can simply say that the solution on the domain of interest $S_\delta(t)$ becomes identically equal to zero and remains zero $\forall t \geqslant t_2$. Therefore, the integration does not need to be continued any further; otherwise, it could only lead to the accumulation of numerical error with time.

The foregoing case may, of course, present only a limited practical interest. The case of central importance will be that of *continuously operating sources*, i.e., when the RHSs to system (1) never cease to operate for $0 < t < +\infty$ while still being supported on the bounded domain $S(t)$ for every $t > 0$. Then, we introduce a smooth partition of unity on the semi-infinite interval $t \geqslant 0$:

$$\forall t \geqslant 0: \qquad \sum_{i=0}^{\infty} \Theta(t - \sigma T i) = 1, \quad \text{supp}\,\Theta(t) \subseteq [-T/2, T/2], \tag{33}$$

where $T > 0$ and $(1/2) \leqslant \sigma < 1$ are parameters, and $\Theta = \Theta(t)$ is a smooth even function. The idea is to have the RHSs of system (1) partitioned accordingly

$$\begin{aligned} \boldsymbol{j}^{(i)}(\boldsymbol{x},t) &= \boldsymbol{j}(\boldsymbol{x},t)\Theta(t-\sigma Ti), \quad \rho^{(i)}(\boldsymbol{x},t) = \rho(\boldsymbol{x},t)\Theta(t-\sigma Ti), \\ \boldsymbol{j}_{\mathrm{m}}^{(i)}(\boldsymbol{x},t) &= \boldsymbol{j}_{\mathrm{m}}(\boldsymbol{x},t)\Theta(t-\sigma Ti), \quad \rho_{\mathrm{m}}^{(i)}(\boldsymbol{x},t) = \rho_{\mathrm{m}}(\boldsymbol{x},t)\Theta(t-\sigma Ti) \end{aligned} \tag{34}$$

so that for each $i = 0, 1, 2, \ldots$ the RHSs (34) be compactly supported on

$$Q_i = \{(\boldsymbol{x},t) | \boldsymbol{x} \in S(t), (\sigma i - 1/2)T \leqslant t \leqslant (\sigma i + 1/2T)\}.$$

Then, each system (1) driven by the RHS (34) for a particular $i$ can be integrated independently using lacunae, starting from $t_0^{(i)} \overset{\text{def}}{=} (\sigma \mathrm{i} - 1/2)\mathrm{T}$ till $t_2^{(i)} \overset{\text{def}}{=} \mathrm{t}_0^{(\mathrm{i})} + \mathrm{T}_{\mathrm{int}} = \mathrm{t}_0^{(\mathrm{i})} + \frac{\mathrm{d}+2\delta+\mathrm{T}}{\mathrm{c}-\mathrm{k}}$, after which its solution becomes identically zero on the domain of interest $S_\delta(t)$. The overall solution can subsequently be obtained by linear superposition. An approach of this type has been successfully implemented in the past for the scalar wave equation [1,2], and for the acoustics system of equations [3]. It provides for the grid convergence that is uniform in time, and also facilitates construction of efficient ABCs.

Unfortunately, a straightforward implementation of this approach to the Maxwell equations may encounter substantial difficulties. Even though the original RHSs of system (1) satisfy Eqs. (2a) and (2b), this may no longer be true for the partitioned RHSs (34). Therefore, the individual Maxwell systems driven by the RHSs (34) for $i = 0, 1, 2, \ldots$ may appear unsolvable.

On the other hand, the auxiliary problem defined in the beginning of this section has been specially designed so that to admit the lacunae-based integration. Indeed, the auxiliary sources given by Theorem 1 satisfy the continuity equations (2a) and (2b) identically, see Corollary 2. If these sources are partitioned according to formulae (34), then for each $i = 0, 1, 2, \ldots$ we will again have $\tilde{\rho}^{(i)} = \tilde{\rho}_{\mathrm{m}}^{(i)} = 0$ and $\mathrm{div}\tilde{\boldsymbol{j}}^{(i)} = \mathrm{div}\tilde{\boldsymbol{j}}_{\mathrm{m}}^{(i)} = 0$, which means that the individual auxiliary sources will independently satisfy the continuity equations (2a) and (2b) for every $i$. Consequently, we may expect that each individual Maxwell system will be uniquely solvable, and that it will be possible to obtain its solution $\boldsymbol{H}^{(i)}$, $\boldsymbol{E}^{(i)}$ on $S_\delta(t)$ with the help of lacunae, i.e., actually compute it on the interval $[t_0^{(i)}, t_2^{(i)}] = [t_0^{(i)}, t_0^{(i)} + T_{\mathrm{int}}]$ and set to zero for all $t > t_2^{(i)}$.

It is also possible to show [1–3] that when reconstructing the overall solution by summing up the individual contributions for each $i = 0, 1, 2, \ldots$

$$\boldsymbol{H}(\boldsymbol{x},t) = \sum_i \boldsymbol{H}^{(i)}(\boldsymbol{x},t), \quad \boldsymbol{E}(\boldsymbol{x},t) = \sum_i \boldsymbol{E}^{(i)}(\boldsymbol{x},t) \tag{35}$$

the resulting sums will, in fact, contain only a finite fixed number of terms that will not increase as the time elapses. The reason is that for any given moment of time, no fragment of the RHS (34) that corresponds to later times can contribute to the solution due to the conventional causality. Besides, no fragment from sufficiently far behind in time can contribute to the solution either, because the domain of interest will be inside the lacuna, i.e., all the waves for a given retarded source will have left $S_\delta(t)$. In addition, each nontrivial term that is present in the sums (35) only needs to be computed on the finite interval $T_{\mathrm{int}}$ that also does not increase as the time elapses. As demonstrated in [1–3], these considerations translate into the temporally uniform grid convergence for any consistent and stable finite-difference scheme. In other words, the accuracy of the numerical solution will not deteriorate with time, i.e., there will be no long-term error buildup.

Moreover, for any given $i = 0, 1, 2, \ldots$ no wave can travel in space further away than the distance $cT_{\mathrm{int}}$ from the boundary of the domain $S(t_0^{(i)})$ during the time interval $T_{\mathrm{int}}$. Therefore, we will have $\boldsymbol{H}^{(i)}(\boldsymbol{x},t) = \boldsymbol{0}$ and $\boldsymbol{E}^{(i)}(\boldsymbol{x},t) = \boldsymbol{0}$ for $\mathrm{dist}\,[\boldsymbol{x}, S(t_0^{(i)})] > cT_{\mathrm{int}}$ and $t_0^{(i)} \leqslant t \leqslant t_2^{(i)}$. As such, instead of the free unobstructed space outside $S(t)$ we may consider outer boundaries with arbitrary (reflecting) properties for solving each of the

individual Maxwell systems for $i = 0, 1, 2, \ldots$ As long as none of these boundaries is located closer than $cT_{\text{int}}$ to $S(t_0^{(i)})$, the solution $\boldsymbol{H}^{(i)}$, $\boldsymbol{E}^{(i)}$ inside $S_\delta(t)$ is not going to feel their presence for $t_0^{(i)} \leqslant t \leqslant t_2^{(i)}$. Furthermore, instead of requiring that no wave may reach an outer boundary before $t = t_2^{(i)}$ we can introduce an even weaker requirement that no reflected wave may come back and reach $S_\delta(t)$ before $t = t_2^{(i)}$. The latter consideration easily translates into the estimate for the minimal distance between $S_\delta(t)$ and the allowed location of any outer boundary, see [1,2]: $Z_{\min} = \frac{c+k}{2} T_{\text{int}}$. In other words, to obtain the correct solution of the auxiliary problem on the domain of interest $S_\delta(t)$ for all $t \geqslant 0$ using representation (35), each individual solution $\boldsymbol{H}^{(i)}$, $\boldsymbol{E}^{(i)}$ may only need to be computed on a bounded auxiliary domain of the maximum size

$$Z = \text{diam } S_\delta(t) + 2Z_{\min} = d + 2\delta + (c + k)T_{\text{int}}. \tag{36}$$

## 4. Artificial boundary conditions for the Maxwell equations

The original formulation of the problem as outlined in Section 2 involves some possibly complex phenomena/processes confined to a bounded region $S(t)$ that manifest themselves by the radiation of electromagnetic waves in the far field, i.e., in $\mathbb{R}^3 \setminus S(t)$. The far-field solution is governed by the homogeneous Maxwell equations. The overall problem is assumed uniquely solvable. By definition, the ABCs should (equivalently) replace the entire exterior homogeneous part of the problem and thus enable actually solving it only on the interior domain $S(t)$. The literature on the subject of ABCs is broad, and we refer the reader to the review papers [30–32]. The ABCs' approach proposed in this paper fits into the general theoretical framework of [33].

The first step is to decompose the original problem into the interior and auxiliary sub-problems. The interior problem is posed on $S(t)$ and inherits all the phenomena and processes that are going on inside this domain. Its formulation, of course, will not be complete unless supplemented by a closure at the boundary $\partial S(t)$. The role of the ABCs is precisely to provide this closure, so that in the ideal case the solution computed on $S(t)$ using the ABCs coincide with the corresponding fragment of the original infinite-domain solution. Using the language of wave physics, one can say that the ABCs on $\partial S(t)$ should simulate the vacuum that extends to infinity and that the bounded domain $S(t)$ is immersed in, so that all the waves generated inside $S(t)$ and traveling toward the boundary $\partial S(t)$ can propagate right through and leave this domain completely, without producing any spurious non-physical effects.

The auxiliary problem for the Maxwell equations was formulated in Section 3. It is posed on the entire space $\mathbb{R}^3$, it is linear and has constant coefficients everywhere, and it is driven by the solenoidal currents and zero charges that exist on $S(t) \setminus S_\varepsilon(t)$ according to Theorem 1. *The key idea of setting the ABCs* is to use the solution of the auxiliary problem right outside $S(t)$ to provide the closure, i.e., the missing boundary data, for the interior problem on $S(t)$. The auxiliary problem, in its own turn, is not fully specified either, because according to Corollary 3 the boundary traces of both fields are needed in order to obtain its source terms. In the framework of setting the ABCs, these traces will be taken from the solution to the interior problem, thereby making the two sub-problems interconnected: The auxiliary sources are constructed based on the interior solution, and the closure for the interior formulation is provided by the solution to the auxiliary problem.

This entire agenda will be implemented directly on the discrete level, thus completely eliminating the two common stages in constructing the ABCs – first obtaining the continuous boundary conditions, and then building their discrete approximation, see [31]. The feasibility of this agenda basically hinges on two essential considerations. The first one has to do with the replacement of non-constructive steps in the proof of Theorem 1 and Corollary 3 by more manageable alternatives. In this paper, it will only be done for a particular cylindrically symmetric setting so that to enable conducting the proof-of-concept computations,

see Section 5; while a more general setup will be addressed later [4]. The second one has to do with the solution of the auxiliary problem. The key point is that even though it is formally posed on an unbounded region (the entire space $\mathbb{R}^3$), the auxiliary problem still lends itself to the actual numerical solution with the help of lacunae, as described in Section 3. In so doing, the computational domain only needs to have a finite size $Z$ of (36), the numerical error does not build up even for long integration times, and the computer expenses per unit time interval remain fixed and non-growing, see [1–3].

The lacunae-based solution algorithm described in Section 3 can even be simplified. In general, for each component $i = 0, 1, 2, \ldots$ of the partitioned sources, the corresponding individual Maxwell system is supposed to be solved on its own auxiliary domain of size $Z$, see (36), centered around $S(t_0^{(i)})$. Instead, we can consider one and the same universal periodic setup with the period $Z$ in each direction. The motion of $S(t)$ will then have to be interpreted as motion on a three-dimensional toroidal surface. Due to the periodicity, for any location of $S(t_0^{(i)})$ on this toroidal surface, there will be exactly $Z_{\min}$ surrounding space in each direction, see formula (36), so that the waves that leave $S(t)$ will not be able to re-enter $S_\delta(t)$ before the time $T_{\text{int}}$ elapses. Therefore, the solution reconstructed on $S_\delta(t)$ will be the same as the one obtained by the algorithm of Section 3 (see [1] for a detailed argument along these lines).

Assume now that there is a space–time grid $\mathbb{N} \times \mathbb{T}$ on the auxiliary domain of size $Z$, see (36), on which a discrete approximation to the auxiliary problem is built. The spatial grid $\mathbb{N}$ consists of the nodes $\boldsymbol{n}$, whereas the temporal grid $\mathbb{T}$ is composed of the time levels $l = 0, 1, 2, \ldots$. The grid $\mathbb{N}$ does not have to offer any special features to accommodate the shape of the domain $S(t)$; it is most convenient to use a uniform Cartesian grid. This grid will be needed for computing the ABCs. Note that the interior problem solved inside $S(t)$ does not have to be approximated on the same grid. For example, in our work on global ABCs for external flow problems [34], we have used a curvilinear grid inside the computational domain, this grid was fitted to the given aerodynamic shape (say, a wing), whereas the ABCs were computed on the auxiliary Cartesian grid. In electromagnetics, the interior grid may also be curvilinear, to reflect, for example, the shape of a given scatterer. In such a case, some data exchange between the interior and auxiliary grids is obviously required; it is typically rendered through interpolations. In the current paper, however, we will restrict ourselves to the simplest case when the interior problem is integrated on the same grid $\mathbb{N}$.

Let $\mathbb{N}^l$, $l = 0, 1, 2, \ldots$, be the time levels of the grid $\mathbb{N} \times \mathbb{T}$, and $\mathbb{S}_{\boldsymbol{n}}^l$ be the $(m+1)$-level stencil of an explicit scheme associated with the node $(\boldsymbol{n}, l) \in \mathbb{N} \times \mathbb{T}$:

$$\mathbb{S}_{\boldsymbol{n}}^l \cap \{\mathbb{N} \times \mathbb{T}\} \subset \{\mathbb{N}^l \cup \mathbb{N}^{l-1} \cup \cdots \cup \mathbb{N}^{l-m}\} \quad \text{and} \quad \mathbb{S}_{\boldsymbol{n}}^l \cap \mathbb{N}^l = (\boldsymbol{n}, l).$$

Introduce the following grid subsets ($h$ is the spatial grid size):

$$\begin{aligned} &\mathbb{N}_+^l = \{(\boldsymbol{n}, l) \in \mathbb{N}^l \cap S(t^l)\}, \\ &\mathbb{N}_+ = \mathbb{N}_+^0 \cup \mathbb{N}_+^1 \cup \mathbb{N}_+^2 \cup \cdots, \\ &\tilde{\mathbb{N}}_+ = \bigcup_{(\boldsymbol{n},l)\in\mathbb{N}_+} \mathbb{S}_{\boldsymbol{n}}^l, \\ &\gamma = \tilde{\mathbb{N}}_+ \setminus \mathbb{N}_+, \end{aligned} \tag{37}$$

$\mathbb{N}_+$ of (37) is the interior sub-grid. The set $\gamma = \gamma^0 \cup \gamma^1 \cup \gamma^2 \cup \cdots$ is called *the grid boundary*; it is a narrow fringe of grid nodes that follows the geometry of $\partial S(t)$. We will require that the domain $S_\delta(t)$, see Fig. 1, be chosen so that $\forall t^l : \tilde{\mathbb{N}}_+^l \subset S_\delta(t^l)$. The parameter $\delta$ can therefore be taken small, about a few grid sizes depending on the structure of the specific $\mathbb{S}_{\boldsymbol{n}}^l$.

We will now describe one time step of the combined interior/auxiliary time-marching algorithm that involves setting the discrete ABCs at $\partial S(t)$.

**Algorithm 4** (ABCs). Let the solution be known on $\tilde{\mathbb{N}}_+$ up to the level $l$.
(A) Perform one interior time step and obtain the solution on $\mathbb{N}_+^{l+1}$;
(B) use the interior solution on $S(t) \setminus S_e(t)$ for time levels up to $t^{l+1}$ and obtain the auxiliary solenoidal currents $\tilde{\boldsymbol{j}}$ and $\tilde{\boldsymbol{j}}_{\mathrm{m}}$ that exist by Theorem 1;
(C) perform one auxiliary time step and supply the solution on $\gamma^{l+1}$.

Clearly, upon completion of part (C) of Algorithm 4 the procedure cyclically repeats itself, i.e., part (A) can be done on the next time level, because $\mathbb{N}_+^{l+1} \cup \gamma^{l+1} = \tilde{\mathbb{N}}_+^{l+1}$, see (37). This way, the computation can be run for as long as necessary, and the closure for the interior problem, i.e., the boundary data on $\gamma$, will always be provided from the solution to the auxiliary problem. Part (B) of Algorithm 4 is to be performed directly on the grid. In the following Section 5, we describe the corresponding implementation for a special case that requires the use of the vector potential $\boldsymbol{A}$, see (29), whereas the general case that employs the solenoidal auxiliary currents constructed using special Taylor expansions will be described in the next paper [4]. Note that in Algorithm 4, when the solution in part (A) is advanced one time level till $l+1$, the auxiliary sources in part (B) are also advanced one time level, but they may be "lagging behind" by a fixed number of levels, depending on the actual scheme and stencil $\mathbb{S}_{\boldsymbol{n}}^{l}$ used. Finally, the time-marching of the auxiliary problem required in part (C) of Algorithm 4 is performed using lacunae, see Section 3. As has been mentioned, this enables integration on the auxiliary domain of a fixed size, and implies only finite non-growing computer expenses per time step.

## 5. Numerical demonstrations

In this section, we conduct a series of computations with the key objective of corroborating our central theoretical finding. In other words, we want to experimentally demonstrate that employing the compactly supported solenoidal currents of Section 2 in the capacity of the source terms for the auxiliary problem would completely clear the way toward the use of lacunae-based ABCs for the Maxwell equations. The computational setup is chosen so that to provide for the easiest, most straightforward, and least expensive implementation, rather than to demonstrate the full generality of the approach. Namely, we employ cylindrical coordinates $(r,\theta,z)$ and assume axial symmetry so that all the quantities depend only on $r$, $z$, and $t$, and $\frac{\partial}{\partial\theta}(\cdot) \equiv 0$. This facilitates the split of system (1) into two independent subsystems such that each governs three out of the total of six field components. The subsystem that connects $E_\theta$, $H_r$, and $H_z$ is referred to as transverse-magnetic (TM); it contains three unsteady equations [cf. Eqs. (1)]

$$\begin{aligned}
&\frac{1}{c}\frac{\partial E_\theta}{\partial t} - \left(\frac{\partial H_r}{\partial z} - \frac{\partial H_z}{\partial r}\right) = -\frac{4\pi}{c} j_\theta,\\
&\frac{1}{c}\frac{\partial H_r}{\partial t} - \frac{\partial E_\theta}{\partial z} = -\frac{4\pi}{c} j_{\mathrm{m}_r},\\
&\frac{1}{c}\frac{\partial H_z}{\partial t} + \frac{1}{r}\frac{\partial (rE_\theta)}{\partial r} = -\frac{4\pi}{c} j_{\mathrm{m}_z}
\end{aligned} \tag{38a}$$

supplemented by the steady-state equation

$$\frac{1}{r}\frac{\partial (rH_r)}{\partial r} + \frac{\partial H_z}{\partial z} = 4\pi\rho_{\mathrm{m}}. \tag{38b}$$

The other steady-state equation of (1), $\operatorname{div}\boldsymbol{E} = 4\pi\rho$, does not appear in the TM system because $\frac{\partial}{\partial\theta}(E_\theta) \equiv 0$. It is rather a part of the other subsystem known as transverse-electric (TE); the latter is not discussed here.

The magnetic currents and charges on the RHSs of Eqs. (38a) and (38b) should always satisfy the continuity equation [cf. formula (2b)]:

$$\frac{\partial \rho_{\mathrm{m}}}{\partial t}+\frac{1}{r}\frac{\partial (r j_{\mathrm{m}_r})}{\partial r}+\frac{\partial j_{\mathrm{m}_z}}{\partial z}=0. \tag{39}$$

In the TM context, there is no continuity equation for the electric currents and charges. The reason is that the only type of electric sources that appear in the TM mode is the current component $j_\theta$, for which we obviously have $\frac{\partial j_\theta}{\partial \theta}\equiv 0$. The electric continuity equation appears in the TE context.

The TM part of the Coulomb gauge definition (29) is given by

$$H_r=-\frac{\partial A_\theta}{\partial z},\quad H_z=\frac{1}{r}\frac{\partial (rA_\theta)}{\partial r},\quad E_\theta=-\frac{1}{c}\frac{\partial A_\theta}{\partial t},\quad \frac{\partial A_\theta}{\partial \theta}\equiv 0 \tag{40}$$

which means that everything is controlled by only one quantity $A_\theta$.

Axial symmetry will allow us to take full advantage of the crucial three-dimensional effects in an essentially two-dimensional computational setting. Besides, construction of the auxiliary sources can be simplified in this case.

As shown in Section 3, the key to using lacunae for integration of the Maxwell equations lies in selecting the RHSs of a special structure that removes the restrictions imposed by the continuity equations. Theorem 1 guarantees existence of these special auxiliary sources – solenoidal currents and corresponding zero charges, but does not offer a full constructive recipe of how they can actually be built. In the cylindrically symmetric TM mode, however, the form of Eqs. (38a), (38b) and the presence of only one continuity equation (39) instead of two suggest that we merely need to guarantee the solenoidal nature of the magnetic currents $\tilde{\boldsymbol{j}}_{\mathrm{m}}$, because $\frac{\partial j_\theta}{\partial \theta}\equiv 0$ anyway. Therefore, the extension of the electric field $E_\theta$ inwards, i.e., from $\mathbb{R}^3\setminus S(t)$ to $S(t)\setminus S_\varepsilon(t)$, that is to be obtained for the purpose of building the auxiliary sources following the proof of Theorem 1, has to be smooth but may otherwise be quite arbitrary. As far as the magnetic auxiliary sources, they still have to be constructed in a special way, so that to ensure $\tilde{\rho}_{\mathrm{m}}=0$ and $\mathrm{div}\tilde{\boldsymbol{j}}_{\mathrm{m}}=\frac{1}{r}\frac{\partial (r\tilde{j}_{\mathrm{m}_r})}{\partial r}+\frac{\partial \tilde{j}_{\mathrm{m}_z}}{\partial z}\equiv 0$, which implies degeneration of the continuity equation (39), cf. Corollary 2. However, the fact that in the TM mode the electric part presents no restriction makes the latter task much easier to accomplish.

Indeed, in this case, if we know the vector potential $\boldsymbol{A}=\boldsymbol{A}(\boldsymbol{x},t)$ (which, like any other quantity in the model, does not depend on $\theta$), we can use it directly rather than look for $\boldsymbol{W}_A(\boldsymbol{x},t)$: $\boldsymbol{A}=\mathrm{curl}\,\boldsymbol{W}_A$ (see the discussion around Eq. (29) that follows the proof of Theorem 1 and Corollary 3). In other words, we can define the extended magnetic field on $\mathbb{R}^3$, $t>0$, as simply $\tilde{\boldsymbol{H}}=\mathrm{curl}\,(\mu\tilde{\boldsymbol{A}})$, where $\tilde{\boldsymbol{A}}(\boldsymbol{x},t)$ is the Whitney extension of the vector potential from $\mathbb{R}^3\setminus S(t)$ into $S(t)\setminus S_\varepsilon(t)$ and $\mu$ is the multiplier of (24). Substitution of this $\tilde{\boldsymbol{H}}$ into the first pair of Maxwell's equations (1) immediately yields $\tilde{\rho}_{\mathrm{m}}=0$ and $\mathrm{div}\tilde{\boldsymbol{j}}_{\mathrm{m}}=0$. For the electric sources, however, if we did not have the axial symmetry this approach would not, generally speaking, allow us to make sure that $\tilde{\rho}=0$ and $\mathrm{div}\tilde{\boldsymbol{j}}=0$, because if we defined the extended electric field as $\tilde{\boldsymbol{E}}=-\frac{1}{c}\frac{\partial(\mu\tilde{\boldsymbol{A}})}{\partial t}$, cf. second equality (29), then it would not necessarily be solenoidal. On the other hand, in the cylindrical TM context this constraint is lifted as the only component of the electric field present, $E_\theta$, can be extended into $S(t)\setminus S_\varepsilon(t)$ arbitrarily, because $\frac{\partial \tilde{E}_\theta}{\partial\theta}=0$ always implies $\frac{\partial \tilde{j}_\theta}{\partial\theta}=0$, and the equation $\mathrm{div}\,\tilde{\boldsymbol{E}}=4\pi\tilde{\rho}$ in this case reduces again to $\frac{\partial \tilde{E}_\theta}{\partial\theta}=0$, i.e., $\tilde{\rho}=0$.

As such, we are going to exploit the vector potential to obtain the solenoidal auxiliary currents needed for numerical experiments, and we will use the gauge definition (40), which is specific for the coordinate system used and the type of symmetry present. The gauge (40) indicates that it is sufficient to build an extension only for $A_\theta$. If we smoothly extend $A_\theta$ from $\mathbb{R}^3\setminus S(t)$ to $S(t)\setminus S_\varepsilon(t)$ and get $\tilde{A}_\theta$, then the modified magnetic field components can be obtained as

$$\tilde{H}_r=-\frac{\partial(\mu\tilde{A}_\theta)}{\partial z},\quad \tilde{H}_z=\frac{1}{r}\frac{\partial(r\mu\tilde{A}_\theta)}{\partial r} \tag{41}$$

and we will clearly have $\operatorname{div}\tilde{\boldsymbol{H}} = \frac{1}{r}\frac{\partial(r\tilde{H}_r)}{\partial r} + \frac{\partial \tilde{H}_z}{\partial z} \equiv 0$ so that the continuity equation (39) will degenerate as required. To our major advantage, in the two-dimensional $(r,z)$ setting (as opposed to a full 3D), the quantity $A_\theta$ can be easily reconstructed by contour integration of the magnetic field using the first two equations of (40). In so doing, the most natural way to build the extension $\tilde{A}_\theta$ and to guarantee its smoothness across the interface $\partial S(t)$ is to apply the same idea right inside $S(t)$ as well, i.e., to simply reconstruct the vector potential on $S(t) \setminus S_\varepsilon(t)$ by contour integration of the interior solution $(H_r, H_z)$. Subsequently, the multiplier $\mu$ is applied to $\tilde{A}_\theta$, the modified magnetic field is derived according to (41), and finally the magnetic auxiliary currents are obtained by applying the Maxwell operators. The situation with the electric auxiliary currents is even more straightforward, as any smooth extension $\tilde{E}_\theta$, once it has been multiplied by $\mu$ and substituted into the corresponding Maxwell equation, yields the desired $\tilde{j}_\theta$. In particular, the interior electric field itself can be used as $\tilde{E}_\theta$ on $S(t) \setminus S_\varepsilon(t)$, which obviously guarantees the smoothness of $\tilde{E}_\theta$ across $\partial S(t)$.

In the discrete framework, all the foregoing operations are done on the grid. The first step is obviously to choose the scheme for the integration of the Maxwell equations (38a). We have employed a version of the well-known Yee scheme [35] adopted for the cylindrical geometry; it is an explicit second-order central-difference staggered solver, which is written as follows on the uniform rectangular $(r,z)$ grid with sizes $\Delta r$ and $\Delta z$ and time step $\Delta t$:

$$\begin{aligned}
&\frac{1}{c}\frac{E^{l+1}_{\theta_{i,j}} - E^{l}_{\theta_{i,j}}}{\Delta t} + \frac{H^{l+\frac{1}{2}}_{z_{i+\frac{1}{2},j}} - H^{l+\frac{1}{2}}_{z_{i-\frac{1}{2},j}}}{\Delta r} - \frac{H^{l+\frac{1}{2}}_{r_{i,j+\frac{1}{2}}} - H^{l+\frac{1}{2}}_{r_{i,j-\frac{1}{2}}}}{\Delta z} = -\frac{4\pi}{c} j^{l+\frac{1}{2}}_{\theta_{i,j}},\\
&\frac{1}{c}\frac{H^{l+\frac{1}{2}}_{r_{i,j+\frac{1}{2}}} - H^{l-\frac{1}{2}}_{r_{i,j+\frac{1}{2}}}}{\Delta t} - \frac{E^{l}_{\theta_{i,j+1}} - E^{l}_{\theta_{i,j}}}{\Delta z} = -\frac{4\pi}{c} j^{l}_{\mathrm{m}_r i,j+\frac{1}{2}},\\
&\frac{1}{c}\frac{H^{l+\frac{1}{2}}_{z_{i+\frac{1}{2},j}} - H^{l-\frac{1}{2}}_{z_{i+\frac{1}{2},j}}}{\Delta t} + \frac{1}{r_{i+\frac{1}{2}}}\frac{r_{i+1}E^{l}_{\theta_{i+1,j}} - r_i E^{l}_{\theta_{i,j}}}{\Delta r} = -\frac{4\pi}{c} j^{l}_{\mathrm{m}_z i+\frac{1}{2},j}.
\end{aligned} \tag{42}$$

Note that the steady-state equation (38b) will not be needed for the actual time marching because the degenerate continuity equation (39) implies that $\operatorname{div}\boldsymbol{H}$ will always preserve its initial value, which is zero. Also note that both Eq. (38a) and the scheme (42) are only valid away from the axis of symmetry $r = 0$. The special treatment needed at the axis is based on the natural consideration that all the quantities involved must be continuous and bounded. For the vector components $E_\theta$ and $H_r$ this requirement, along with the axial symmetry, implies that both $E_\theta$ and $H_r$ must be equal to zero at $r = 0$. The same will obviously be true for $j_\theta$ and $j_{\mathrm{m}_r}$. For the vector component $H_z$, which is parallel to the axis of symmetry, the same arguments lead to the conclusion that $\frac{\partial H_z}{\partial r}|_{r=0} = 0$. Next, for $r \ll 1$ we have: $E_\theta(r,\cdot) = E'_\theta(0,\cdot)r + o(r)$ and consequently, $\frac{1}{r}\frac{\partial(rE_\theta)}{\partial r} = \frac{1}{r}\frac{\partial(r^2 E'_\theta(0,\cdot))}{\partial r} + \mathrm{o}(1)$, which means that $\frac{1}{r}\frac{\partial(rE_\theta)}{\partial r}|_{r=0} = 2\frac{\partial E_\theta}{\partial r}|_{r=0}$. Therefore, for $r = 0$ system (38a) transforms into

$$\begin{aligned}
&E_\theta(0,z,t) = 0,\\
&H_r(0,z,t) = 0,\\
&\frac{1}{c}\frac{\partial H_z}{\partial t} + 2\frac{\partial E_\theta}{\partial r} = -\frac{4\pi}{c} j_{\mathrm{m}_z}.
\end{aligned} \tag{43}$$

Discretization of (43) consistent with (42) reads

$$\begin{aligned} &E^l_{\theta_{0,j}} = 0, \\ &H^{l+\frac{1}{2}}_{r_{0,j+\frac{1}{2}}} = 0, \\ &\frac{1}{c}\frac{H^{l+\frac{1}{2}}_{z_{\frac{1}{2},j}} - H^{l-\frac{1}{2}}_{z_{\frac{1}{2},j}}}{\Delta t} + \frac{2}{\Delta r}E^l_{\theta_{1,j}} = -\frac{4\pi}{c}j^l_{\mathrm{m}_{z\frac{1}{2},j}} \end{aligned} \tag{44}$$

provided that the grid line $i = 0$ coincides with the axis $r = 0$. Finally, the discrete counterpart of the Coulomb gauge (40) is given by

$$\begin{aligned} &H^{l+\frac{1}{2}}_{r_{i,j+\frac{1}{2}}} = -\frac{A^{l+\frac{1}{2}}_{\theta_{i,j+1}} - A^{l+\frac{1}{2}}_{\theta_{i,j}}}{\Delta z}, \quad H^{l+\frac{1}{2}}_{z_{i+\frac{1}{2},j}} = \frac{1}{r_{i+\frac{1}{2}}}\frac{r_{i+1}A^{l+\frac{1}{2}}_{\theta_{i+1,j}} - r_iA^{l+\frac{1}{2}}_{\theta_{i,j}}}{\Delta r}, \\ &E^l_{\theta_{i,j}} = -\frac{1}{c}\frac{A^{l+\frac{1}{2}}_{\theta_{i,j}} - A^{l-\frac{1}{2}}_{\theta_{i,j}}}{\Delta t}. \end{aligned} \tag{45}$$

Further detail on the specific computational setup that we have used can be found in our report [36]. It involves a compact source of unsteady electromagnetic radiation engaged in a straightforward motion (along the $z$ axis). The motion itself is not uniform either and consists of repeated acceleration/deceleration cycles. There is an analytic reference solution, against which we compare the numerical results obtained on a sequence of subsequently more fine grids. This allows us to experimentally judge the grid convergence. The integration in time is conducted till $100 \cdot \frac{d}{c}$, which is equal to one hundred times the interval required for the waves to cross the domain $S(t)$ of fixed diameter $d$. The shape of this domain $S(t)$ is chosen spherical, while the grid is rectangular, and no adaptation is required.

The scheme (42), (44) is used for independently marching both the interior solution inside $S(t)$ and the solution of the auxiliary problem. Algorithm 4 renders coupling between the two solutions. On every time step, the first two equations of (45) are used for reconstructing the discrete vector potential $\tilde{A}^{l+\frac{1}{2}}_{\theta_{i,j}}$ in the transition region $S(t) \setminus S_\varepsilon(t)$, which basically amounts to integrating the discrete interior solution for the magnetic field along the coordinate lines of the grid. The reconstructed potential is needed on stage (B) of Algorithm 4. It is first modified by applying $\mu$ of (24), then the modified fields are obtained by using the discrete version of (41), which is the same as the first two equations of (45), and finally, the auxiliary sources are obtained by applying the operators on the left-hand side of (42).

In Fig. 2 we present the computational error for $E_\theta$ as it depends on time on the three grids that we have employed. The error was evaluated in the maximum norm on the domain $S(t)$. We see that the algorithm provides for no long-term error buildup, and also that it displays the design second-order grid convergence. Error profiles for both magnetic field components $H_r$ and $H_z$ look practically the same and we are not showing them here.

Let us now discuss how the performance of the lacunae-based ABCs is affected by the key parameter involved – the width of the transition region $S(t) \setminus S_\varepsilon(t)$. This width $\varepsilon$ obviously reflects on how well the smooth extensions and smooth multiplier function $\mu(\boldsymbol{x}, t)$ are resolved on the grid, and as such, how smooth the auxiliary RHSs will effectively be. The latter, in turn, affect the quality of the discrete lacunae, i.e., how sharp the aft fronts of the waves really are in the discrete framework. Besides having a potential effect on the error behavior, the width of the transition region also determines how many grid nodes are needed to support the auxiliary RHSs. Those RHSs basically control the extent of temporal nonlocality of the lacunae-based ABCs. The algorithm requires keeping them on the interval of length $T_{\mathrm{int}}$ that immediately precedes the current moment of time, and as such, the more narrow the transition region is, the less additional storage is needed.

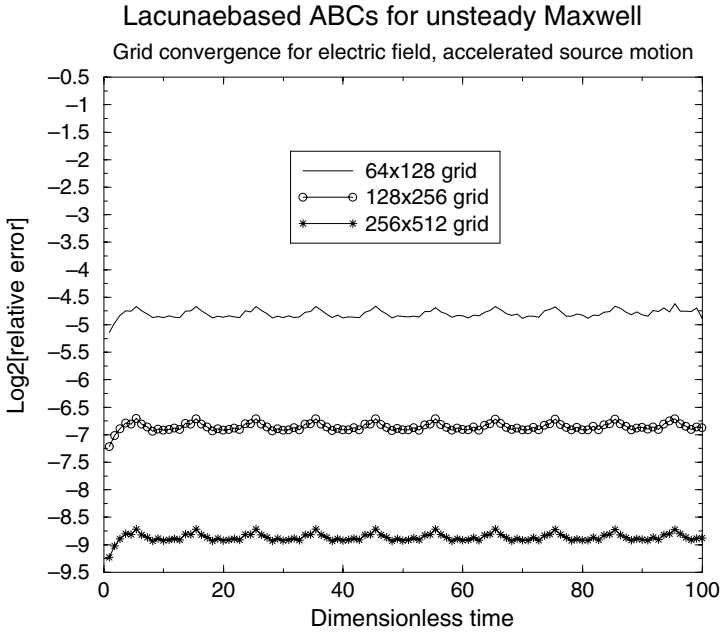


Fig. 2. Grid convergence study with lacunae-based ABCs, $\varepsilon = 10\Delta r$.

The error curves in Fig. 2 were obtained for the transition region $S(t) \setminus S_\varepsilon(t)$ being relatively wide, on the order of 10 grid cell sizes. In so doing, the actual geometric width of $S(t) \setminus S_\varepsilon(t)$ decreases with the refinement of the grid. We are, however, interested to find out what happens when the number of cells in the transition region also decreases. In Figs. 3–6 we are showing the $E_\theta$ error profiles for the width of the transition region being $\varepsilon = 8, 6, 4$, and 2 grid cell sizes, respectively.

We observe that with the decrease of $\varepsilon$ the error deteriorates, which is natural to expect. We also notice, though, that the deterioration is more visible on the coarser grids, whereas on the finest grid that we have employed, $256 \times 512$, it is much slower. Qualitatively, this is the same type of behavior as we have seen in acoustics, see [3]. There is, however, an important difference as well. In acoustics, when $\varepsilon$ decreases, all the error profiles start to grow more or less monotonically with time, see [3]. The smaller the $\varepsilon$ the faster this growth is, although on the finest grid it is not as fast as on the coarser grids. In contradistinction to that, in the current electromagnetic context the error profile on the finest grid always remains flat on some initial time interval, after which it starts to deteriorate. The extent of this initial interval decreases with the decrease of $\varepsilon$, but even for the narrowest transition region that we have considered, $\varepsilon = 2\Delta r$, it is still quite substantial, about 30 units, i.e., 30 times the time needed for the waves to cross the domain, see Fig. 6. The presence of this initial flat portion of the error profile is beneficial as it essentially means that the lacunae-based ABCs can be used for a certain period of time *with no deterioration of performance* even when the auxiliary RHSs involved are not really smooth. We note that having only two grid sizes across $S(t) \setminus S_\varepsilon(t)$ does imply that there is no smoothing in the transition region at all. We are rather having a sharp truncation, and effectively substituting an equivalent of the Heaviside function on the grid for the multiplier $\mu(\boldsymbol{x}, t)$.

As of yet, we cannot offer a rigorous theoretical explanation of why the algorithm appears more sensitive to the quality of the discrete lacunae on coarser grids than on the fine grid. To some extent this is counterintuitive because a typical instability would rather manifest itself by a rapid deterioration of the solution

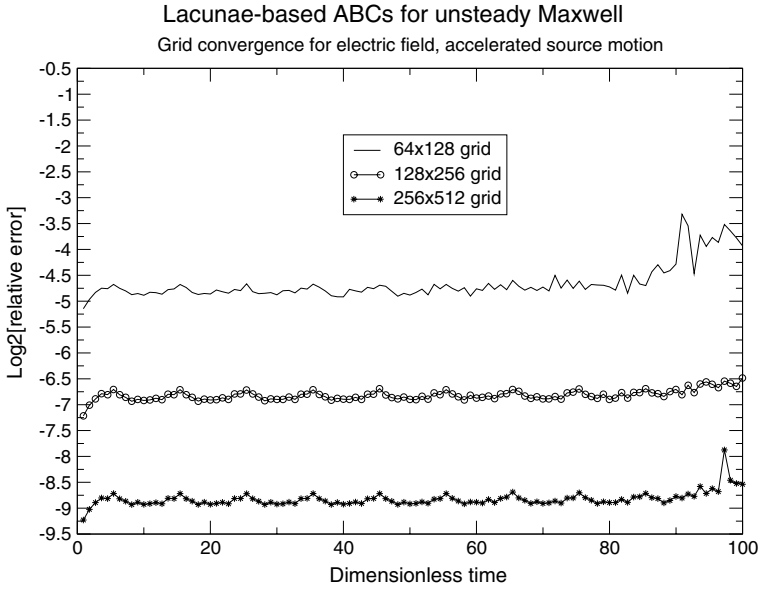


Fig. 3. Grid convergence study with lacunae-based ABCs, $\varepsilon = 8\Delta r$.

when the grid is refined. We can only "speculate" that the observed behavior has to do with the actual magnitude of those discrete "tails" behind the aft fronts of the waves that are due to the "imperfections" in the auxiliary sources, and that apparently are still smaller on fine grids. Altogether, this phenomenon is

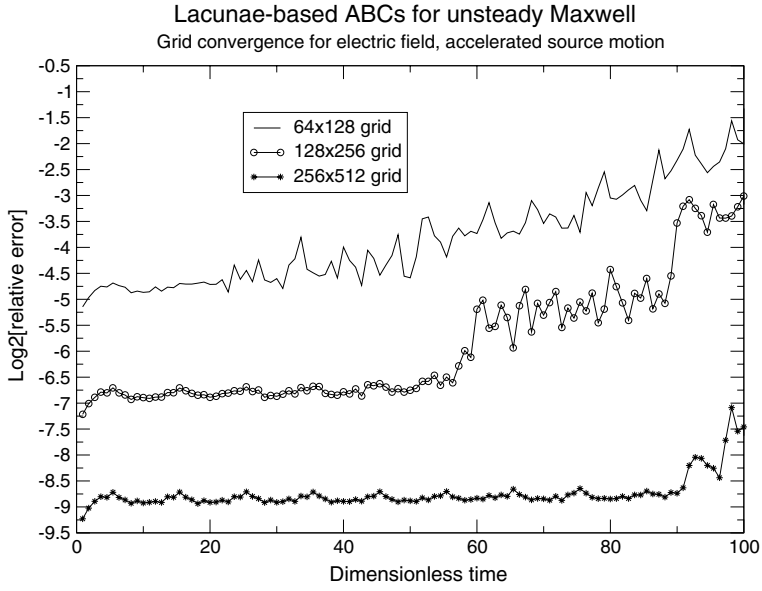


Fig. 4. Grid convergence study with lacunae-based ABCs, $\varepsilon = 6\Delta r$.

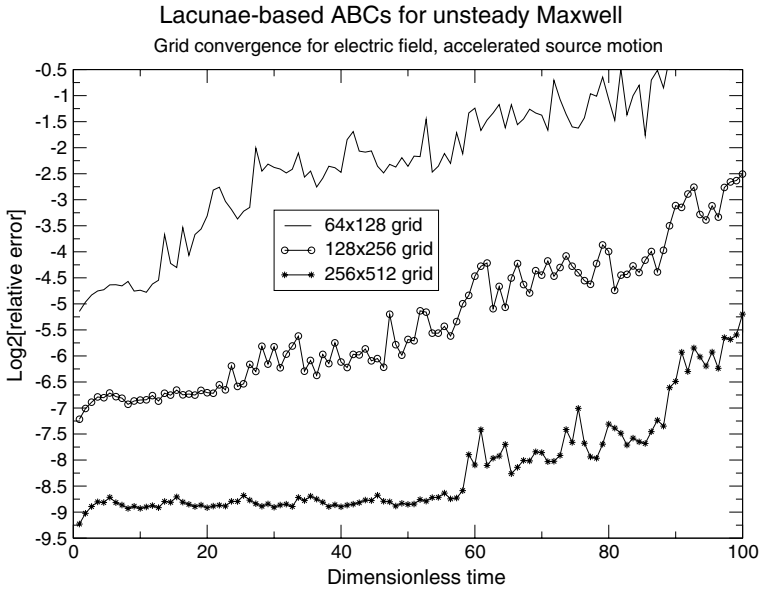


Fig. 5. Grid convergence study with lacunae-based ABCs, $\varepsilon = 4\Delta r$.

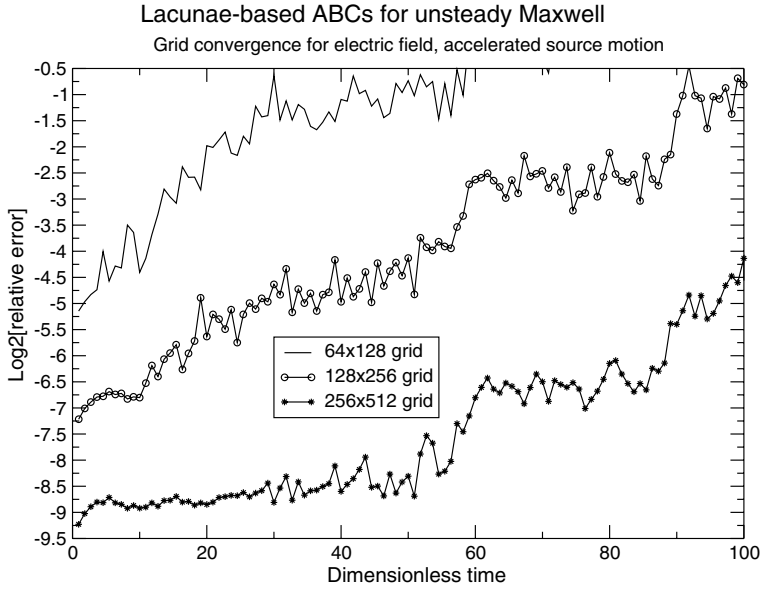


Fig. 6. Grid convergence study with lacunae-based ABCs, $\varepsilon = 2\Delta r$.

certainly advantageous for computations with lacunae-based ABCs, because fine grids are needed for high overall accuracy anyway, and at the same time they will allow to maintain high accuracy of the boundary treatment for longer periods of time.

## 6. Discussion

We have identified the requirement of continuity of the charges and currents as a key obstacle for applying the previously proposed lacunae-based methods [1–3] to Maxwell's equations. We have also been able to show that there are special auxiliary sources – zero charges and solenoidal currents – that satisfy this requirement identically and as such, eliminate the corresponding restrictions. This paves the way toward constructing and testing the algorithm for setting highly accurate global artificial boundary conditions for the computation of time-dependent electromagnetic waves.

In general, the lacunae-based ABCs are obtained directly for the discrete formulation of the problem and can complement any consistent and stable finite-difference scheme. In so doing, neither a rational approximation of non-reflecting kernels [31], nor discretization of the continuous boundary conditions is required. The extent of temporal nonlocality of these ABCs appears fixed and limited, which is not a result of any approximation but rather a direct consequence of the fundamental properties of the solution. The proposed ABCs can handle artificial boundaries of irregular shape on regular grids with no fitting/adaptation needed. Besides, they possess a unique capability of being able to handle boundaries of moving computational domains, including the case of accelerated motion.

In the current paper, we have only built the electromagnetic lacunae-based ABCs for a specially chosen simple setting that involves cylindrically symmetric TM Maxwell's equations. We have also been able to experimentally verify their theoretical design properties on a series of the proof-of-concept computations. Implementation for a more general setting will follow in the forthcoming paper [4].

## References

[1] V.S. Ryaben'kii, S.V. Tsynkov, V.I. Turchaninov, Long-time numerical computation of wave-type solutions driven by moving sources, Appl. Numer. Math. 38 (2001) 187–222.
[2] V.S. Ryaben'kii, S.V. Tsynkov, V.I. Turchaninov, Global discrete artificial boundary conditions for time-dependent wave propagation, J. Comput. Phys. 174 (2) (2001) 712–758.
[3] S.V. Tsynkov, Artificial boundary conditions for the numerical simulation of unsteady acoustic waves, J. Comput. Phys. 189 (2) (2003) 626–650.
[4] S.V. Tsynkov, On the application of lacunae-based methods to Maxwell's equations: Part II (in progress).
[5] L.D. Landau, E.M. Lifshitz, The Classical Theory of Fields, Pergamon Press, Oxford, 1962.
[6] P.M. Morse, H. Feshbach, Methods of Theoretical Physics. Parts I and II, McGraw-Hill, Boston, 1953.
[7] O.A. Ladyzhenskaya, The Mathematical Theory of Viscous Incompressible Fluid, second ed., Gordon and Breach, New York, 1969.
[8] E.M. Stein, Singular Integrals and Differentiability Properties of Functions, Princeton University Press, Princeton, NJ, 1970.
[9] A.J. Devaney, Nonuniqueness in the inverse scattering problem, J. Math. Phys. 19 (7) (1978) 1526–1531.
[10] A.J. Devaney, G.C. Sherman, Nonuniqueness in inverse source and scattering problems, IEEE Trans. Antennas Propag. AP-30 (5) (1982) 1034–1037, see also comments by N.N. Bojarski and those by W.R. Stone, as well as the authors' replies, on pages 1037–1042.
[11] H.E. Moses, The time-dependent inverse source problem for the acoustic and electromagnetic equations in the one- and three-dimensional cases, J. Math. Phys. 25 (6) (1984) 1905–1923.
[12] H.E. Moses, R.T. Prosser, Initial conditions, sources, and currents for prescribed time-dependent acoustic and electromagnetic fields in three dimensions. I. The inverse initial value problem. Acoustic and electromagnetic "bullets", expanding waves, and imploding waves, IEEE Trans. Antennas Propag. 34 (2) (1986) 188–196.
[13] A.J. Devaney, E. Wolf, Radiating and nonradiating classical current distributions and the fields they generate, Phys. Rev. D 8 (4) (1973) 1044–1047.
[14] I. Petrowsky, On the diffusion of waves and the lacunas for hyperbolic equations, Matematicheskii Sbornik (Recueil Mathématique) 17 (59) (3) (1945) 289–370.
[15] V.S. Vladimirov, Equations of Mathematical Physics, Dekker, New York, 1971.
[16] R. Courant, D. Hilbert, in: Methods of Mathematical Physics, vol. II, Wiley, New York, 1962.
[17] J. Hadamard, Lectures on Cauchy's Problem in Linear Partial Differential Equations, Yale University Press, New Haven, 1923.
[18] J. Hadamard, Problème de Cauchy, Hermann et cie, Paris, 1932 (in French).

[19] J. Hadamard, The problem of diffusion of waves, Ann. Math. 43 (2) (1942) 510–522.
[20] M.F. Atiyah, R. Bott, L. Gårding, Lacunas for hyperbolic differential operators with constant coefficients. I, Acta Math. 124 (1970) 109–189.
[21] M.F. Atiyah, R. Bott, L. Gårding, Lacunas for hyperbolic differential operators with constant coefficients. II, Acta Math. 131 (1973) 145–206.
[22] M. Matthisson, Le probléme de Hadamard relatif á la diffusion des ondes, Acta Math. 71 (1939) 249–282 (in French).
[23] K.L. Stellmacher, Ein Beispiel einer Huyghensschen Differentialgleichung, Nachr. Akad. Wiss. Göttingen. Math. Phys. Kl. Math. – Phys. Chem. Abt. 1953 (1953) 133–138 (in German).
[24] J.E. Lagnese, K.L. Stellmacher, A method of generating classes of Huygens' operators, J. Math. Mech. 17 (1967) 461–472.
[25] K.L. Stellmacher, Eine Klasse huyghenscher Differentialgleichungen und ihre Integration, Math. Ann. 130 (1955) 219–233 (in German).
[26] R. Schimming, A review of Huygens' principle for linear hyperbolic differential equations, in: Proceedings of the IMU Symposium "Group-Theoretical Methods in Mechanics", Novosibirsk, USSR, 1978, USSR Acad. Sci., Siberian Branch, Novosibirsk, 1978.
[27] M. Belger, R. Schimming, V. Wünsch, A survey on Huygens' principle, Z. Anal. Anwendungen 16 (1) (1997) 9–36, dedicated to the memory of Paul Günther.
[28] P. Günther, Huygens' principle and hyperbolic equations, in: Perspectives in Mathematics, vol. 5, Academic Press, Boston, MA, 1988, with appendices by V. Wünsch.
[29] P. Günther, Ein Beispiel einer nichttrivialen Huygensschen Differentialgleichung mit vier unabhängigen Variablen, Arch. Rational Mech. Anal. 18 (1965) 103–106 (in German).
[30] D. Givoli, Non-reflecting boundary conditions, J. Comput. Phys. 94 (1991) 1–29.
[31] T. Hagstrom, Radiation boundary conditions for the numerical simulation of waves, in: A. Iserlis (Ed.), Acta Numerica, vol. 8, Cambridge University Press, Cambridge, 1999, pp. 47–106.
[32] S.V. Tsynkov, Numerical solution of problems on unbounded domains. A review, Appl. Numer. Math. 27 (1998) 465–532.
[33] V.S. Ryaben'kii, Nonreflecting time-dependent boundary conditions on artificial boundaries of varying location and shape, Appl. Numer. Math. 33 (2000) 481–492.
[34] S.V. Tsynkov, External boundary conditions for three-dimensional problems of computational aerodynamics, SIAM J. Sci. Comp. 21 (1999) 166–206.
[35] K.S. Yee, Numerical solution of initial boundary value problem involving Maxwell's equations in isotropic media, IEEE Trans. Antennas Propag. 14 (1966) 302–307.
[36] S.V. Tsynkov, Artificial boundary conditions for the numerical simulation of unsteady electromagnetic waves, Technical Report CRSC-TR03-19, Center for Research in Scientific Computation, North Carolina State University, Raleigh, NC, April 2003.